that cyst form ameba often disappears spontaneously without any treatment [28,29]. There is controversy about the need for cyst eradication following metronidazole or tinidazole treatment, especially in endemic areas where re-infection is frequent. In this study, recurrence of IA within the first year of metronidazole treatment was noted in only two patients of 82 patients who did not receive luminal therapy. Moreover, long-term follow-up indicated IA recurrence also in those who received luminal agents, and the benefits obtained from luminal treatment seemed to have disappeared. IA recurred more frequently in those with HCV infection, which was recently reported to be transmittable sexually among MSM [30], and in those who acquired new syphilis infection during the follow-up period, suggesting that sexually active MSM tend to experience IA recurrence due to re-acquisition of new *E. histolytica* infection. HBV exposure and positive TPHA at IA diagnosis did not correlate with IA recurrence probably because the high prevalence of these two parameters in this study masked the difference between recurrence and non-recurrence cases. Educational approach for safer sex may be more appropriate rather than luminal treatment to prevent IA recurrence after treatment.

Eleven genetic strains of *E. histolytica* were identified in this study and none of them had been reported so far from geographic areas other than Japan [21,22,31,32], indicating that diverse Japan-specific isolates of *E. histolytica* are already prevalent among MSM in Japan. In fact, the *E. histolytica* seropositivity rate in HIV-1-infected MSM in our clinic was as high as 17.9% in 2009 (unpublished data), which is comparable with the seropositivity rate in Japanese MSM reported more than 20 years ago [5]. Unfortunately, we could not compare the genotypes of *E. histolytica* between the incidences of the primary and recurrent IA within the same individuals due to the lack of appropriate stocked samples, which would have probably demonstrated acquisition of new infection.

Considered together, the results emphasize the difficulty of preventing IA recurrence without educational approach to prevent new amebic infection even after successful IA treatment in the high risk groups such as HIV-1-infected MSM. The spread of *E. histolytica* in MSM of other developed countries beyond Asia should be of great concern.

Supporting Information

Table S1 Patient demographics with and without luminal treatment.
(DOC)

Table S2 Genotyping data of 6 STR loci in 14 clinical samples.
(DOC)

Author Contributions

Conceived and designed the experiments: HG JT SO. Performed the experiments: KW AEdC TN. Analyzed the data: KW HG. Contributed reagents/materials/analysis tools: KW HG JT SO. Wrote the paper: KW HG.

References

1. Walsh JA (1986) Problems in recognition and diagnosis of amebiasis: estimation of the global magnitude of morbidity and mortality. Rev Infect Dis 8: 228–238.
2. Haque R, Huston CD, Hughes M, Houpt E, Petri WA, Jr. (2003) Amebiasis. N Engl J Med 348: 1565–1573.
3. Takeuchi T, Kobayashi S, Asami K, Yamaguchi N (1987) Correlation of positive syphilis serology with invasive amebiasis in Japan. Am J Trop Med Hyg 36: 321–324.
4. Takeuchi T, Miyahira Y, Kobayashi S, Nozaki T, Motta SR, et al. (1990) High seropositivity for *Entamoeba histolytica* infection in Japanese homosexual men: further evidence for the occurrence of pathogenic strains. Trans R Soc Trop Med Hyg 84: 250–251.
5. Takeuchi T, Okuzawa E, Nozaki T, Kobayashi S, Mizokami M, et al. (1989) High seropositivity of Japanese homosexual men for amebic infection. J Infect Dis 159: 808.
6. Ohnishi K, Kato Y, Imamura A, Fukayama M, Tsunoda T, et al. (2004) Present characteristics of symptomatic *Entamoeba histolytica* infection in the big cities of Japan. Epidemiol Infect 132: 57–60.
7. Ohnishi K, Murata M (1997) Present characteristics of symptomatic amebiasis due to *Entamoeba histolytica* in the east-southeast area of Tokyo. Epidemiol Infect 119: 363–367.
8. Liu CJ, Hung CC, Chen MY, Lai YP, Chen PJ, et al. (2001) Amebic liver abscess and human immunodeficiency virus infection: a report of three cases. J Clin Gastroenterol 33: 64–68.
9. Park WB, Choe PG, Jo JH, Kim SH, Bang JH, et al. (2007) Amebic liver abscess in HIV-infected patients, Republic of Korea. Emerg Infect Dis 13: 516–517.
10. Hung CC, Chen PJ, Hsieh SH, Wong JM, Fang CT, et al. (1999) Invasive amoebiasis: an emerging parasitic disease in patients infected with HIV in an area endemic for amoebic infection. AIDS 13: 2421–2428.
11. Hung CC, Deng HY, Hsiao WH, Hsieh SM, Hsiao CF, et al. (2005) Invasive amebiasis as an emerging parasitic disease in patients with human immunodeficiency virus type 1 infection in Taiwan. Arch Intern Med 165: 409–415.
12. Hung CC, Ji DD, Sun HY, Lee YT, Hsu SY, et al. (2008) Increased risk for *Entamoeba histolytica* infection and invasive amebiasis in HIV seropositive men who have sex with men in Taiwan. PLoS Negl Trop Dis 2: e175.
13. Chen YM, Kuo SH (2007) HIV-1 in Taiwan. Lancet 369: 623–625.
14. van Griensven F, de Lind van Wijngaarden JW (2010) A review of the epidemiology of HIV infection and prevention responses among MSM in Asia. AIDS 24: S30–40.
15. Lee JH, Kim GJ, Choi BS, Hong KJ, Keo MK, et al. (2010) Increasing late diagnosis in HIV infection in South Korea: 2000-2007. BMC Public Health 10: 411.
16. Annual surveillance report of HIV/AIDS in Japan, 1997 (1999) AIDS Surveillance Committee, Ministory of Health and Welfare, Japan. Working Group of Annual AIDS Surveillance, Ministry of Health and Welfare, Japan. Jpn J Infect Dis 52: 55–87.
17. Tsai JJ, Sun HY, Ke LY, Tsai KS, Chang SY, et al. (2006) Higher seroprevalence of *Entamoeba histolytica* infection is associated with human immunodeficiency virus type 1 infection in Taiwan. Am J Trop Med Hyg 74: 1016–1019.
18. Powell SJ, MacLeod I, Wilmot AJ, Elsdon-Dew R (1966) Metronidazole in amoebic dysentery and amoebic liver abscess. Lancet 2: 1329–1331.
19. Powell SJ, Maddison SE, Elsdon-Dew R (1966) Rapid faecal transmission and invasive amoebiasis in Durban. S Afr Med J 40: 646–649.
20. Hsu MS, Hsieh SM, Chen MY, Hung CC, Chang SC (2008) Association between amebic liver abscess and human immunodeficiency virus infection in Taiwanese subjects. BMC Infect Dis 8: 48.
21. Ali IK, Zaki M, Clark CG (2005) Use of PCR amplification of tRNA gene-linked short tandem repeats for genotyping *Entamoeba histolytica*. J Clin Microbiol 43: 5842–5847.
22. Escueta-de Cadiz A, Kobayashi S, Takeuchi T, Tachibana H, Nozaki T (2010) Identification of an avirulent *Entamoeba histolytica* strain with unique tRNA-linked short tandem repeat markers. Parasitol Int 59: 75–81.
23. Stanley SL, Jr. (2003) Amoebiasis. Lancet 361: 1025–1034.
24. Irusen Em, Jackson TF, Simjee AE (1992) Asymptomatic intestinal colonization by pathogenic *Entamoeba histolytica* in amebic liver abscess: prevalence, response to therapy, and pathogenic potential. Clin Infect Dis 14: 889–893.
25. Blessmann J, Tannich E (2002) Treatment of asymptomatic intestinal *Entamoeba histolytica* infection. N Engl J Med 347: 1384.
26. McAuley JB, Herwaldt BL, Stokes SL, Becher JA, Roberts JM, et al. (1992) Diloxanide fumarate for treating asymptomatic *Entamoeba histolytica* cyst passers: 14 years' experience in the United States. Clin Infect Dis 15: 464–468.
27. McAuley JB, Juranek DD (1992) Paromomycin in the treatment of mild-to-moderate intestinal amebiasis. Clin Infect Dis 15: 551–552.
28. Ruiz-Palacios GM, Castanon G, Bojalil R, Tercero E, Rausser S, et al. (1992) Low risk of invasive amebiasis in cyst carriers. A longitudinal molecular seroepidemiological study. Arch Med Res 23: 289–291.
29. Blessmann J, Ali IK, Nu PA, Dinh BT, Viet TQ, et al. (2003) Longitudinal study of intestinal Entamoeba histolytica infections in asymptomatic adult carriers. J Clin Microbiol 41: 4745–4750.
30. van de Laar TJ, Matthews GV, Prins M, Danta M (2010) Acute hepatitis C in HIV-infected men who have sex with men: an emerging sexually transmitted infection. AIDS 24: 1799–1812.
31. Tawari B, Ali IK, Scott C, Quail MA, Berriman M, et al. (2008) Patterns of evolution in the unique tRNA gene arrays of the genus Entamoeba. Mol Biol Evol 25: 187–198.
32. Ali IK, Solaymani-Mohammadi S, Akhter J, Roy S, Gorrini C, et al. (2008) Tissue invasion by Entamoeba histolytica: evidence of genetic selection and/or DNA reorganization events in organ tropism. PLoS Negl Trop Dis 2: e219.

J Antimicrob Chemother 2012; **67**: 375–386
doi:10.1093/jac/dkr484 Advance Access publication 22 November 2011

Journal of Antimicrobial Chemotherapy

Transcriptional and functional analysis of trifluoromethionine resistance in *Entamoeba histolytica*

Gil M. Penuliar[1–3], Atsushi Furukawa[1,2], Kumiko Nakada-Tsukui[1], Afzal Husain[1,2], Dan Sato[4] and Tomoyoshi Nozaki[1,5]*

[1]Department of Parasitology, National Institute of Infectious Diseases, Toyama 1-23-1, Shinjuku-ku, Tokyo 162-8640, Japan; [2]Department of Parasitology, Gunma University Graduate School of Medicine, 3-39-22 Showa-machi, Maebashi 371-8511, Japan; [3]Institute of Biology, College of Science, University of the Philippines, Diliman, Quezon City 1101, Philippines; [4]Institute for Advance Biosciences, Keio University, Tsuruoka, Yamagata 997-0052, Japan; [5]Graduate School of Life and Environmental Sciences, University of Tsukuba, 1-1-1 Tennodai, Tsukuba, Ibaraki 305-8572, Japan

*Corresponding author. Tel: +81-3-45822690; Fax: +81-3-52851219; E-mail: nozaki@nih.go.jp

Received 10 July 2011; returned 6 September 2011; revised 13 October 2011; accepted 27 October 2011

Objectives: Drug resistance in parasitic protozoa is an obstacle to successful chemotherapy. Understanding how pathogens respond to drugs is crucial in preventing resistance. Previously, we have shown that in *Entamoeba histolytica*, methionine γ-lyase (*Eh*MGL) downregulation results in trifluoromethionine resistance. The transcriptional response, however, of this parasite to the drug is not known. In this study, we used microarray analysis to determine whether additional genes are involved.

Methods: The expression profiles of 9230 genes in wild-type and trifluoromethionine-resistant strains were compared. Episomal overexpression of *Eh*BspA1 was performed to verify its role in trifluoromethionine resistance. The transcriptomes of a trifluoromethionine-resistant strain cultured with or without trifluoromethionine, an *Eh*MGL gene-silenced strain, a strain with reduced susceptibility to metronidazole and a wild-type strain under cysteine-deprived conditions were compared to determine the specificity of the changes observed in the trifluoromethionine-resistant strain.

Results: The expression of 35 genes differed at least 3-fold between trifluoromethionine-resistant and wild-type strains. Some of the genes play roles in metabolism, the stress response and gene regulation. *EhMGL* and *EhBspA1* were found to be highly downregulated and upregulated, respectively. Overexpression of *Eh*BspA1 conferred partial resistance to trifluoromethionine. Comparative transcriptome analysis showed that genes modulated in trifluoromethionine-resistant strains were specific.

Conclusions: *E. histolytica* has few known resistance mechanisms against drugs. In this study, we showed that aside from *Eh*MGL downregulation, induction of *Eh*BspA1 plays a role in trifluoromethionine resistance. We also showed a unique set of induced genes that could represent the signature profile of trifluoromethionine resistance in *E. histolytica*.

Keywords: microarray, methionine γ-lyase, leucine-rich repeat BspA protein

Introduction

Parasitic diseases in man can be controlled, at least in part, by chemotherapeutic drugs. How long this situation will last, however, is a matter for conjecture since drug resistance is becoming an increasing problem.[1–4] Drug resistance occurs in parasitic protozoans by various mechanisms;[5–10] in *Entamoeba histolytica*, the causative agent of amoebic dysentery and liver abscess,[11] *in vitro* studies with emetine and metronidazole have led to the recognition of some basic mechanisms by which *E. histolytica* becomes resistant to these drugs.[6–10] A common mechanism is the efflux system where toxic substances are extruded through specific pumps.[9,10,12] This mechanism is thought to be operative in *E. histolytica* resistant to emetine, where multiple P-glycoprotein genes encoding putative transmembrane channels were shown to have increased expression.[9,10] Metronidazole resistance, on the other hand, has been associated with increased expression of iron-containing superoxide dismutase and peroxiredoxin, and decreased expression of flavin reductase and ferredoxin 1.[6–8] Currently, metronidazole

is still the drug of choice against amoebic infections,[13] but in the event that clinical resistance to this drug becomes prevalent, the lack of an alternative drug would cause major health problems in endemic areas.

Trifluoromethionine (*S*-trifluoromethyl-L-homocysteine) is a halogenated methionine analogue, previously reported to exert antimicrobial activity against anaerobic bacteria and parasitic protozoa such as *E. histolytica* and *Trichomonas vaginalis*.[14–18] Inside the cell, trifluoromethionine is catabolized by methionine γ-lyase (EC 4.4.1.11, *Eh*MGL1/2) into α-keto butyrate, ammonia and trifluoromethanethiol. The last product is unstable under physiological conditions and non-enzymatically converted to carbonothionic difluoride, a potent cross-linker of primary amine groups, by which trifluoromethionine exerts it toxic effects.[17] In 2010, Sato *et al.*,[14] reported the superior cytotoxic effect of trifluoromethionine compared with metronidazole, and that a single administration of trifluoromethionine effectively prevented the formation of amoebic liver abscess in a rodent model. Previously, however, we reported that *E. histolytica* has the capacity to develop resistance against the drug *in vitro*, and that resistance was associated with *Eh*MGL repression.[19]

DNA microarray technology is a powerful tool that can probe the genome on high-density microarrays and analyse the expression profiles of thousands of genes simultaneously.[20–22] To further understand the nature of resistance to trifluoromethionine, we used cDNA microarray technology to examine the mRNA expression of trifluoromethionine-resistant (TFMR) isogenic strains. We compared the results with the transcriptome of TFMR cells cultured in the absence of the drug, with strains targeted for *EhMGL* gene silencing, those selected for metronidazole resistance and those cultured in cysteine-deprived medium; we observed the specific regulation of a set of genes that may represent a signature profile of trifluoromethionine resistance.

Materials and methods

Chemicals, reagents, and drugs

Trifluoromethionine was produced as described previously.[14,15] Metronidazole, L-cysteine, anti-HA-agarose and E-64 (trans-epoxysuccinyl-L-leucylamido-[4-guanidino]butane) were purchased from Sigma-Aldrich (St. Louis, MO, USA). TRIzol Reagent, SuperScript III First-Strand Synthesis System, PLUS reagent, Lipofectamine and geneticin (G418) were acquired from Invitrogen (Carlsbad, CA, USA). All other chemicals were obtained from Wako Pure Chemical (Osaka, Japan) unless otherwise stated. Trifluoromethionine and metronidazole were dissolved in DMSO to a stock concentration of 200 mM and 100 mM, respectively, and stored at −30°C.

Parasites and cultivation

E. histolytica strains HM-1:IMSS cl6 (HM-1) and G3, kindly given by David Mirelman, Weisman Institute, Israel, were cultured axenically in BI-S-33 medium for 48–72 h at 35.5°C in 13 mm×100 mm Pyrex screw cap culture tubes or 25 cm^2 tissue culture flasks (#152094, Nunc, Roskilde, Denmark).[23] Generation and cultivation of TFMR in the presence or absence of trifluoromethionine (*Eh*MGL1gs and *Eh*MGL2gs) were as previously described.[19] Isogenic cells with reduced susceptibility to 8 μM metronidazole were selected following the method outlined by Wassmann *et al.*[7] Trophozoites grown under cysteine-deprived conditions were cultured in BI-S-33 medium without 8 mM L-cysteine supplementation for 24 h as previously described.[24]

RNA isolation

Cells cultured in 25 cm^2 tissue culture flasks were harvested by replacing the spent medium with 10 mL of PBS, pH 7.2, followed by incubation on ice for 10 min. Cell suspension was centrifuged at 500×**g** for 5 min at 4°C and the pellet washed thrice with PBS. Total RNA was extracted with TRIzol Reagent according to the manufacturer's instructions, cleaned with an RNeasy kit (Qiagen, Germany) and assessed for quality with the Experion automated electrophoresis system and Experion RNA StdSens analysis kit (Bio-Rad Laboratories, Inc., Hercules, CA, USA). RNA quantity was determined by measuring the absorbance at 260 nm with a NanoDrop ND-1000 UV-Vis spectrophotometer (NanoDrop Technologies, Wilmington, DE, USA).

Microarray hybridization

Samples from three independent RNA extractions were processed according to standard protocols and by using kits specified in the Affymetrix GeneChip Expression Analysis Technical Manual (P/N 702232 Rev. 3).[25] Briefly, 5 μg of RNA was reverse transcribed to cDNA and used to synthesize biotin-labelled cRNA. After purification, cRNA was fragmented and hybridized onto a probe array chip (Eh_Eia520620F) that was custom made by Affymetrix (Santa Clara, CA, USA).[24,26] Following hybridization, arrays were washed and stained with streptavidin/phycoerythrin (Molecular Probes, Eugene, OR, USA) using an Affymetrix GeneChip Fluidics Station 450. Arrays were scanned with an Affymetrix GeneChip Scanner 3000 at 570 nm. Each array image was visually screened to discard signal artifacts, scratches and debris.

The microarray used in this study was tailored based on information mined from the *E. histolytica* and *Entamoeba invadens* sequences stored at the TIGR and Pathema databases. It contained 9230 probe sets for *E. histolytica* and an additional 25 and 81 control probe sets for *Entamoeba* and Affymetrix, respectively. Nomenclature for the IDs was based on whether the probe set is unique to either TIGR (e.g. 12.m00345) or Pathema (EHI_123456), or is found in both databases (98.m00765_234567). Probe sets labelled with '_at' represent a single gene, while those labelled '_s_at' represent probe sets that share all probes identically with at least two sequences. The '_s_at' probe sets represent highly similar transcripts, shorter forms of alternatively polyadenylated transcripts, or common regions in the 3′ ends of multiple alternative splice forms. Probe sets labeled '_x_at', on the other hand, represent probe sets where it was not possible to select either a unique probe set or a probe set with identical probes among multiple transcripts. Rules for cross-hybridization were excluded in order to design '_x_at' probe sets, therefore these probe sets could cross-hybridize with other genes in an unpredictable manner.[27]

Data normalization and analysis

Raw probe intensities were generated by the GeneChip Operating Software (GCOS) and a GeneTitan Instrument. The resulting expression values were analysed by Genespring GX 10.0.2 to identify differentially expressed genes. Only genes that were considered 'present' by GCOS in at least two arrays were used in further analysis. Correlation coefficients were calculated in Genespring using standard correlation. Probe sets were considered differentially expressed between HM-1 and TFMR if they had at least a 3-fold change and P value <0.05, calculated using Welch's t-test, after multiple test correction by the Benjamini–Hochberg method. A post-hoc test using Tukey's Honestly Significant Difference test was conducted to determine significant differences between samples.

Deduced amino acid sequences of differentially expressed genes were searched against GenBank by using BLAST.[28] Matches against hypothetical proteins with E-value $<10^{-75}$ for BLASTP were considered as putative

orthologues.[29] GO annotations were mined from the Gene Ontology Annotation Database,[30] while the genomic location of each gene was obtained from Pathema-*Entamoeba*.[31] Transmembrane domain prediction was performed using the following online servers: HMMTOP,[32] SOSUI,[33] TMHMM,[34] TopPred,[35] TMpred[36] and Phobius.[37] Signal peptide sequences were predicted using SignalP,[38] SOSUIsignal[39] and Phobius.[37] Putative transmembrane domains and signal peptides were considered valid only if positive hits were found in all servers used. Heatmaps were made using Heatmap Builder[40] while Venn diagrams were constructed using Venn Diagram Generator.[41]

Data deposition

The microarray data reported in this paper has been deposited in the Gene Expression Omnibus (GEO) database[42] with accession number GSE32314.

Quantitative real-time PCR (qRT–PCR)

Total RNA extracted for the microarray was used for qRT-PCR. The synthesis of cDNA was performed using the SuperScript III First-Strand Synthesis System according to the manufacturer's instructions. The cDNA synthesis was completed on a DNA Engine Peltier Thermal Cycler (Bio-Rad Laboratories, Inc., Hercules, CA, USA). The Fast SYBR Green Master Mix (Applied Biosystems, Foster City, CA, USA) was used for qRT-PCR in accordance with the manufacturer's instructions. The list of genes whose expression was verified by qRT-PCR is in Table S1, and includes a housekeeping gene, RNA polymerase II (*Eh*RNAPII), as a control. Each PCR reaction contained 5 μL (1:50 dilution) of cDNA and 15 μL of primer mix, composed of 10 μL of 2× Fast SYBR Green Master Mix, sense and antisense primers and nuclease-free water, to bring the volume to 20 μL. qRT-PCR was performed using a StepOne Plus Real-Time PCR System (Applied Biosystems, Foster City, CA, USA) with the following cycling conditions: enzyme activation at 95°C for 20 s, followed by 40 cycles of denaturation at 95°C for 3 s and annealing/extension at 60°C for 30 s. All test samples were run in triplicate including an RT-negative control for each sample set along with a blank control consisting of nuclease-free water in place of cDNA. Quantification for each target gene was determined by the ΔΔCt method with *Eh*RNAPII as the reference gene.

Generation of transgenic amoeba overexpressing EhBspA1

Full-length *Eh*BspA1 was amplified from TFMR cDNA with sense and antisense primers containing appropriate restriction sites (Table S1). After purification the gene was inserted into an expression plasmid, pEhEx, as previously described.[43] The plasmid was introduced into the G3 strain by lipofection, with minor modifications as previously described.[44] Briefly, 5×10^5 cells suspended in 5 mL of supplemented Opti-MEM medium were seeded into a well in a 12-well plate and incubated under anaerobic condition at 35.5°C for 30 min. Following incubation, 4.5 mL of medium from each well was removed and 500 μL of liposome/plasmid mixture (5 μg of plasmid, 10 μL of PLUS reagent and 20 μL of Lipofectamine in Opti-MEM medium) was added. After 5 h of transfection, cells were harvested by placing the plate on ice for 15 min, then added to culture tubes with 5.5 mL of cold BI-S-33 medium, and incubated at 35.5°C for 24 h. Transformants were initially selected in the presence of 1 μg/mL G418 and drug concentration was gradually increased to 20 μg/mL over the following four weeks before the transformants were analysed.

Immunoblot analysis

Total protein (30 μg) was separated in 12% (w/v) SDS-polyacrylamide gel under reducing conditions and subsequently electrotransferred onto nitrocellulose membranes (Hybond-C Extra; Amersham Biosciences, Little Chalfont, Bucks, United Kingdom). Membranes were blocked by incubation in 5% non-fat dried milk (BD, Le Pnt de Claix, France) in TBST (50 mM Tris-HCl, pH 8.0, 150 mM NaCl and 0.05% Tween 20) for 1.5 h. Blots were reacted with 1:1000 diluted anti-HA mouse monoclonal antibody (Clone 16B12) (Covance, Berkeley, CA, USA) for 1 h. The membranes were washed with TBST and further reacted with 1:1000 alkaline phosphatase-conjugated anti-mouse IgG antibody (New England Biolabs, Beverly, MA, USA) for 1 h. After further washings with TBST, specific proteins were visualized with an alkaline phosphatase conjugate substrate kit (Bio-Rad, Hercules, CA, USA) and scanned with an ImageScanner (Amersham Pharmacia Biotech, Piscataway, NJ, USA). The experiments were repeated in triplicate with protein isolated from two independent extractions.

Measurement of E. histolytica adhesion

Trophozoites in exponential growth phase were harvested, washed with cold PBS, and centrifuged at 500×**g** for 5 min at 4°C. The plate adhesion assay was performed as previously described.[19] Briefly, approximately 1×10^5 trophozoites were seeded into a well of a 96-well plate coated with either human fibronectin (BD BioCoat Cell Environment; BD Biosciences, San Joe, CA, USA) or collagen type I (SigmaScreen; Sigma-Aldrich, St Louis, MO, USA), and incubated under anaerobic conditions using Anaerocult A (Merck, Darmstadt, Germany) for up to 40 min at 35.5°C. The medium was removed and non-adherent cells were gently washed twice with PBS warmed to 35.5°C. Adherent cells were fixed with 40 mg/mL paraformaldehyde (TAAB Laboratories, Aldermaston, England) for 10 min and washed twice with PBS. Cells were stained with 1 mg/mL methylene blue in 100 mM borate buffer, pH 8.7, for 20 min and washed twice with distilled water. The stain was extracted with 200 μL of 20 mg/mL SDS and the absorbance measured at 660 nm using a DU 530 Spectrophotometer (Beckman Coulter, Fullerton, CA, USA).

Immunofluorescence assay

To determine the subcellular location of *Eh*BspA1, transfected amoebae were processed for an indirect immunofluorescence assay. Briefly, amoebae in 6 mL of confluent culture were incubated on ice for 10 min, concentrated by centrifugation at 500×**g** for 5 min and spotted onto an 8 mm well of a glass slide (Wheaton Science Products, Millville, NJ, USA). After incubation at 35.5°C for 15 min, spent medium was removed, and cells were washed with PBS and fixed with 40 mg/mL paraformaldehyde (TAAB Laboratories, Berks, England) for 10 min. Following a further PBS wash, cells were permeabilized and blocked with 0.2% (w/v) saponin in 1% (w/v) BSA in PBS for 10 min, and incubated with 1:1000 monoclonal anti-HA antibody for 1 h. After a PBS wash, cells were reacted with 1:1000 anti-mouse IgG conjugated with Alexa Fluor 488 (Invitrogen, Carlsbad, CA, USA) for 1 h, washed again with PBS and prepared for confocal microscopy, as previously described.[43,44]

Flow cytometry

Transformants for fluorescence-activated cell sorting (FACS) analysis were processed as described in the immunofluorescence assay, except that all procedures were performed in 1.5 mL tubes. A FACS Calibur cytometer (Becton Dickinson, San Jose, CA, USA) was used to run and analyse the samples, as previously described.[45]

Immunoprecipitation

Confluent cultures of *Eh*BspA1-HA and pEhEx control transformants maintained with 20 μg/mL G418 were harvested by centrifugation at 500×**g** for 5 min. Cells were washed twice with cold PBS and 1 mL of lysis buffer [50 mM Tris-HCl, pH 7.5, 150 mM NaCl, 0.5% Triton-X 100, 5% glycerol, complete mini EDTA-free protease inhibitor cocktail (Roche Molecular Biochemicals, Mannheim, Germany) and 200 mM E-64] was added. Cell suspensions were subjected to three freeze–thaw cycles, followed by centrifugation at 12000×**g** for 20 min. Protein (5 μg) was mixed with 50 μL of 50% anti-HA-agarose and incubated at 4°C overnight with mild rotation. Agarose beads were collected by centrifugation at 500×**g** for 3 min and washed four times with 1 mL of lysis buffer at 4°C with rotation for 10 min per wash. HA peptide (60 μL, 400 μg/mL) was added followed by incubation at room temperature for 2 h. Beads and eluate were collected by centrifugation and analysed by SDS-PAGE and immunoblot. Silver staining was performed with a Silver Stain MS Kit according to the manufacturer's instructions.

Results and discussion

Differentially expressed genes in TFMR

The emergence of drug resistance poses a significant obstacle to the success of chemotherapy. In parasitic protozoa, the mechanisms behind the development of resistance are not clearly understood and may arise from a plethora of genetic alterations during repeated exposure to a drug. Previously we have shown that in *E. histolytica* trifluoromethionine resistance results from *Eh*MGL repression.[19] Complete gene inactivation, however, likely does not occur suddenly *in situ*, but develops progressively after continuous exposure to permissive concentrations of a drug. During this time, it is reasonable to assume that a number of processes occur concomitant with *Eh*MGL repression.

To identify other potential genes associated with trifluoromethionine resistance, expression changes in TFMR were analysed by a whole-genome cDNA microarray. The relative ratio of mRNA abundance of 9230 genes (~95% of all annotated amoebic genes) between TFMR and HM-1 was examined for differential expression. Only a limited number of genes showed 3-fold or higher changes in TFMR (63 probe sets; Figure 1, Table S2). The list of genes was narrowed further to 35 (<1.0% of probe sets used) after the removal of redundant genes, probe sets labelled with '_x_at' and NCBI entries considered obsolete after standard genome annotation processing.

Twenty-three of the genes were upregulated, while 12 genes were downregulated (Tables 1 and 2). The most upregulated gene was a member of the leucine-rich repeat (LRR) protein family, designated *Eh*BspA1 (EHI_015120) in this study, which was upregulated 527-fold. Genes encoding tyrosine kinase (EHI_070110), zinc finger protein (EHI_176800), and two hypothetical proteins (EHI_127670 and EHI_092110) were also upregulated by at least 25-fold. The most downregulated genes were *Eh*MGL1 (EHI_144610) and *Eh*MGL2 (EHI_142250), which had changes of 195-fold and 172-fold, respectively. An EF-hand calcium-binding domain-containing protein (EHI_151890) was also downregulated by more than 25-fold. These results support the idea that drug resistance requires the regulation and concerted action of a small number of amoeba proteins, and that genes other than *Eh*MGL play roles, albeit not directly, in trifluoromethionine resistance.

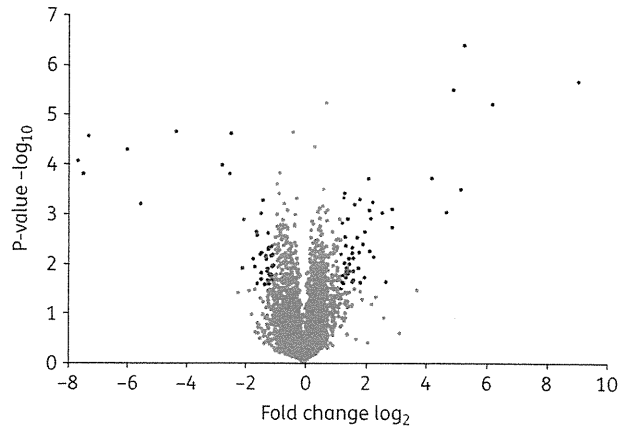

Figure 1. Volcano plot of the differentially expressed genes in TFMR. X-axis is the $\log_2$ ratio of gene expression between TFMR and HM-1; y-axis is $-\log_{10}$ of the adjusted *P* value. Red dots represent differentially expressed genes satisfying $P < 0.05$ and >3-fold expression difference. This figure appears in colour in the online version of *JAC* and in black and white in the printed version of *JAC*.

Comparison with TFMR cultured without trifluoromethionine

Previously, we have shown that long-term culture of TFMR strains in the absence of trifluoromethionine, designated TFMR(−), failed to restore the susceptible phenotype.[19] To determine which of the modulated genes in TFMR were truly important in drug resistance, we compared its transcriptome with that of TFMR(−). We found the same genes to be differentially regulated, with the exception of the amino acid transporter (EHI_190460) and DnaJ family protein (EHI_183280), which were not significantly modulated in TFMR(−) (Figure 2b). This is further evidence that genes listed in Tables 1 and 2 have definite roles in trifluoromethionine resistance. The return to steady-state levels of DnaJ and amino acid transporter, however, is understandable because removal of drug pressure is assumed to alleviate stress. It is possible that trifluoromethionine caused the repression of the promoters of these genes and that its removal caused the return of their expression to HM-1 levels. The possible roles of these two genes in trifluoromethionine resistance are discussed below. Currently, it is not known why more genes were modulated in TFMR(−) (Figure 2a).

Confirmation of differential gene expression by qRT–PCR

Microarray results must be validated by an alternative and complementary gene expression profiling method, and qRT–PCR is the most commonly used technology for this purpose. Figure 3(a) shows a comparison of the differential gene expression for 12 representative genes, with RNA polymerase II as reference. The correlation between microarray and qRT–PCR results demonstrates a reasonable degree of similarity in the pattern of expression for the genes selected for this comparison ($R^2 = 0.8$) (Figure 3b).

Table 1. Genes upregulated in TFMR

Probe set ID	NCBI RefSeq	Gene name	*P* value	Fold-change
EHI_015120_at	XM_643740.2	Leucine rich repeat protein, BspA family	6.1E-09	527
EHI_127670_at	XM_644313.2	Hypothetical protein	4.6E-08	73
EHI_092110_at	XM_649471.1	Hypothetical protein	1.1E-05	35
EHI_070110_at	XM_643743.1	Tyrosine kinase, putative	1.3E-06	30
EHI_176800_at	XM_644747.1	Zinc finger protein, putative	7.9E-05	25
EHI_070120_at	XM_643742.1	Myotubularin, putative	1.8E-05	18
EHI_092100_at	XM_649470.1	Chitinase, putative	4.1E-05	7
EHI_119510_at	XM_646380.1	Hypothetical protein	1.5E-02	5
EHI_045340_s_at	XM_648481.2	Glutamate synthase beta subunit, putative	1.3E-03	4
EHI_073480_at	XM_651584.1	ADP-ribosylation factor, putative	9.4E-03	4
EHI_062740_at	XM_645458.1	Hypothetical protein	1.6E-02	4
EHI_067090_at	XM_643754.2	Hypothetical protein	1.9E-05	3
EHI_117580_at	XM_646500.1	Hypothetical protein	6.1E-04	3
EHI_039590_at	XM_643902.1	O-acyltransferase	6.7E-05	3
EHI_114660_at	XM_645242.1	DENN domain-containing protein 2D	1.9E-03	3
EHI_121470_at	XM_643356.1	DNA methyltransferase, putative	2.6E-03	3
EHI_118410_at	XM_644811.1	Tyrosine kinase, putative	6.6E-03	3
EHI_150420_at	XM_650731.1	Hypothetical protein	7.1E-03	3
EHI_127710_s_at	XM_644310.2	Leucine rich repeat protein, BspA family	4.8E-04	3
EHI_114650_at	XM_645241.2	Hypothetical protein	1.8E-03	3
EHI_021570_at	XM_644909.1	Serine acetyltransferase 1	1.9E-03	3
EHI_166820_at	XM_645437.1	Ulp1 protease family protein	5.0E-03	3
EHI_130860_at	XM_650451.2	Longevity-assurance family protein	3.6E-03	3

Table 2. Genes downregulated in TFMR

Probe set ID	NCBI RefSeq	Gene name	*P* value	Fold change
EHI_144610_at	XM_647004.2	Methionine gamma-lyase	3.4E-06	195
EHI_142250_at	XM_643714.1	Methionine gamma-lyase	7.1E-06	172
EHI_151890_at	XM_652298.1	EF-hand calcium-binding domain containing protein	3.2E-06	62
EHI_103470_at	XM_647325.1	Hypothetical protein	1.0E-03	7
EHI_031640_at	XM_648447.2	Sulfotransferase	2.2E-04	6
EHI_155630_at	XM_650686.2	Hypothetical protein	5.1E-04	3
EHI_088600_s_at	XM_001914535.1	Ribosomal protein S30, putative	3.1E-02	3
EHI_075640_at	XM_001914030.1	Phosphatase domain-containing protein	8.7E-04	3
EHI_183280_at	XM_650378.2	DnaJ family protein	3.4E-03	3
EHI_195250_at	XM_643195.1	AIG1 family protein	3.4E-03	3
EHI_005030_at	XM_647743.1	Hypothetical protein	1.9E-04	3
EHI_190460_at	XM_646352.1	Amino acid transporter, putative	1.2E-02	3

Functional analysis

Based on GO annotations, the open reading frames (ORFs) of the identified genes encode proteins potentially involved in metabolism, signalling, vesicular trafficking and gene regulation (Table S3). Some genes, however, are without GO annotations, such as the two LRR BspA genes and a number of hypothetical proteins. While the GO annotations may be applicable for a variety of processes, genes in the same annotations may be the ones most essential in allowing cells to survive during the initial drug treatment. The functional significance of these changes and their relationship to the response to trifluoromethionine can only be explained by taking into account the relevant roles that they play in the control of key gene functions, such as metabolism and signal transduction.

Very few of the differentially expressed genes encode potential membrane proteins. Only 9 (26%) of the genes contained 1 to 12 transmembrane domains (Table S4). Seven of these were upregulated while two were downregulated. Two genes presumably encode proteins with tyrosine kinase activity, while one encodes an amino acid transporter. Proteins encoded by five genes have predicted signal peptides (Table S4), while two additional genes are predicted to encode proteins with signal

peptides but without transmembrane domains (chitinase, EHI_092100; hypothetical protein, EHI_117580).

When we examined the genomic locations of these genes, we found that most of the genes were encoded on different scaffolds, while eight genes formed pairs that occupied the same contig (Table S5). Two pairs, however, were located on opposite strands, but the members of each pair were regulated in the same manner. Fold changes for pairs found on the same strand were almost the same, while for those lying on opposite strands, the difference in fold changes was as high as 24. The distance between genes lying on the same strand was less than 640 bases; it was therefore possible for these genes to have the same regulatory elements.

Downregulation of EhMGL

*Eh*MGL catalyses the single-step degradation of sulphur-containing amino acids into ammonia, α-keto acids and volatile thiols such as methanethiol.[46] It has been implicated in the degradation of trifluoromethionine in *E. histolytica*,[15] and previously we have shown that *Eh*MGL repression results in trifluoromethionine resistance.[19] The differential expression of *Eh*MGL1 and *Eh*MGL2 in this study confirms our previous report. While it is assumed that *Eh*MGL may not be essential in amoebae growing in a nutrient-rich environment (which is why its repression was tolerated), its downregulation is not without consequences. It is possible that complete lack of *Eh*MGL activity also leads to trifluoromethionine resistance indirectly through its role in metabolism and growth. Without *Eh*MGL activity, TFMR strains lose one means of producing α-keto acids, i.e. pyruvate and butyrate, which are needed to form acetyl-CoA and α-propionic acid. Lower concentrations of these compounds would have an effect on energy production and growth.[47] While statistically comparable, the growth of TFMR strains is slightly slower than that of HM-1 as previously reported, and this growth defect is even more evident in the *Eh*MGL gene-silenced strains.[19] This slower growth hints at the importance of *Eh*MGL, and, at the same time, may have been a survival strategy, as discussed below.

Overexpression of EhBspA1

E. histolytica encodes a family of BspA-like surface proteins composed of 75 members.[48] In bacteria, these proteins are expressed on the cell surface and promote adhesion to and invasion of epithelial cells.[49,50] In this study, two *Eh*BspA genes were upregulated in TFMR, one of which is not expressed in HM-1 (EHI_015120, designated *Eh*BspA1 in this study) based on qRT-PCR and RT-PCR (Figure 3; Figure 4a). We took this as an indication of its having an important role in trifluoromethionine resistance. To test this hypothesis, we created and characterized an *Eh*BspA1 overexpresser and identified its effector molecule. The expression of *Eh*BspA1 was confirmed by immunoblot against anti-HA antibody and qRT-PCR (Figure 4a and b). Immunofluorescence assay of the *Eh*BspA1 overexpressor showed that it is localized in the cytoplasm (Figure 4c). This was verified by cell fractionation followed by immunoblot (data not shown). The results were consistent with its apparent lack of a transmembrane domain and signal peptide (Table S4). It was therefore not surprising that overexpression of the gene did not

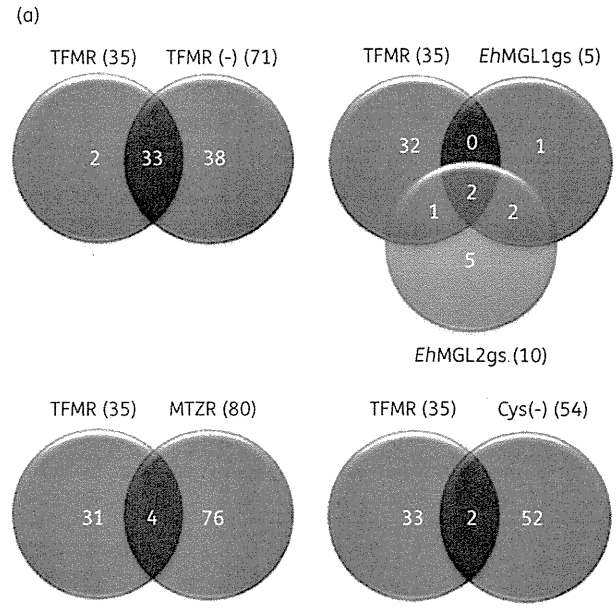

Figure 2. (a) Venn diagrams showing the overlap of differentially expressed genes in TFMR with TFMR(−), *Eh*MGL1gs, *Eh*MGL2gs, MTZR, and Cys(−). (b) Comparative fold change analysis of differentially expressed genes in TFMR to those of TFMR (−), *Eh*MGL1gs, *Eh*MGL2gs, MTZR and Cys(−), indicates that the modulation of the genes was specific to TFMR. Black dots indicate upregulated genes, while green dots indicate downregulated genes. Dot diameter is proportional to fold change. This figure appears in colour in the online version of *JAC* and in black and white in the printed version of *JAC*.

increase the adhesive capacity of the transformant (Figure 4d). In contrast, we previously showed that TFMR cells adhere more strongly than HM-1.[19]

*Eh*BspA1 was partially resistant to trifluoromethionine compared with the pEhEx control (Figure 4e). IC_{50} values of the drug against the *Eh*BspA1 overexpresser and the control were 25.1 μM and 13.8 μM, respectively. FACS analysis also showed that there was an increase, albeit low, in signal intensity when *Eh*BspA1 was exposed to trifluoromethionine (Figure S1a). While the level of expression of *Eh*BspA1 in BspA1-HA was significantly higher than with pEhEx-HA (Figure 4b), the mRNA concentration we determined for TFMR was seven times greater (Figure 3a). It is conceivable that the low level of resistance in *Eh*BspA1-HA compared with TFMR was partly due to the large difference in *Eh*BspA1 expression. It should be noted, however, that the partial drug resistance and increased signal intensity observed in *Eh*BspA1-HA was not due to a decrease in *Eh*MGL activity, as was determined by immunoblot using anti-*Eh*MGL antibody (Figure S1b).

A key feature of the BspA protein is a leucine-rich repeat (LRR) motif known to mediate protein-protein interactions.[51] The capacity of LRR proteins to interact with many ligands enables them to contribute to important cellular functions ranging from the regulation of the cell cycle to protein trafficking and signal transduction.[52] Through immunoprecipitation, we identified S-phase kinase-associated protein 1 (Skp1; EHI_134960) as the binding

(b)

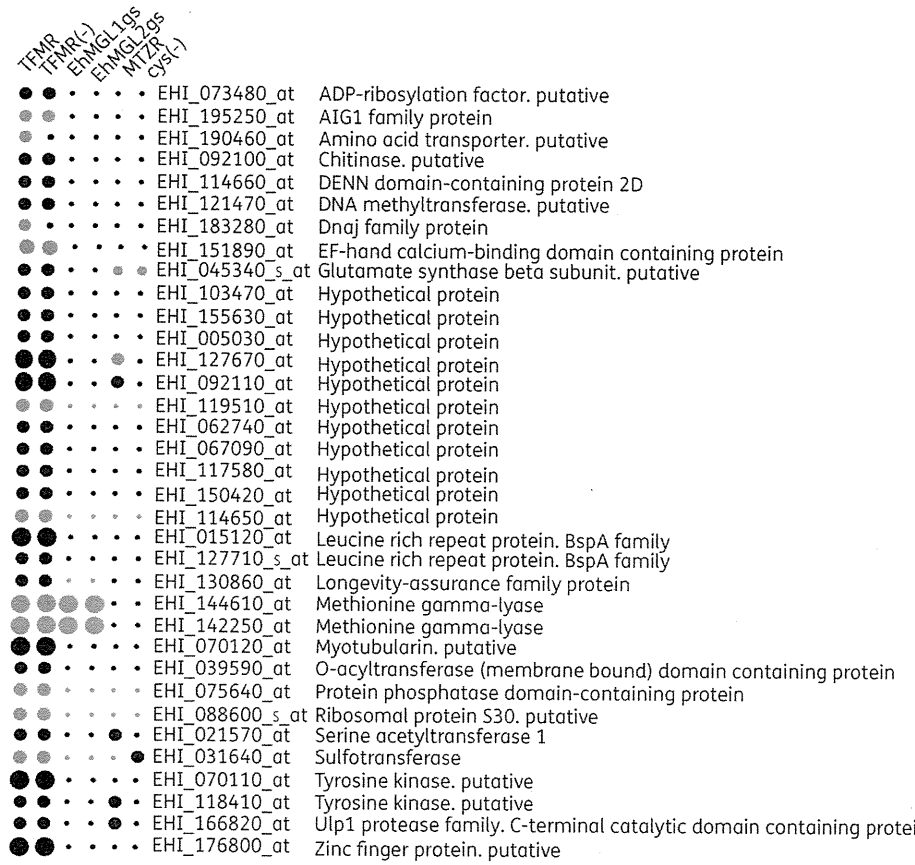

Figure 2. Continued.

protein of *Eh*BspA1 (Figure S1c). In yeasts, Skp1 forms multiple protein complexes implicated in cell division,[53] induction of protective gene expression[54] and multidrug resistance.[55] It is possible that overexpression of *Eh*BspA1 preceded the downregulation of *Eh*MGL, and was important during the early stages of drug selection.

Genes involved in metabolism, stress and nucleic acid binding

The generation time of TFMR strains is longer than that of HM-1.[19] This phenotype may have resulted as a survival strategy through alterations in the activity of the metabolic genes listed in Tables 1 and 2. In cancer cells it has been shown that growth-stimulated cells are more susceptible to drugs because they have less time for DNA repair.[56,57] A longer generation time would therefore be advantageous, as that would provide TFMR with the opportunity to prevent or repair damage, and may also allow more potent mechanisms of resistance to emerge over time. This may be the reason behind the downregulation of ribosomal protein S30 (EHI_088600) and sulfotransferase (EHI_031640), the latter of which has been shown to be important in the activation of a range of compounds.[58] The amino acid transporter (EHI_190460) identified in this study could be a potential transporter of trifluoromethionine.[14] It is possible that the gene was downregulated to prevent trifluoromethionine access to the cell, similarly to what has been seen in *Trypanosoma brucei*, where a loss of function in the amino acid transporter encoded by TbAAT6 resulted in eflornithine resistance.[5] DnaJ (EHI_183280) expression, on the other hand, is associated with enhanced susceptibility to chemotherapeutics in ovarian carcinoma,[59] which might account for its downregulation in TFMR.

The upregulation of chitinase (EHI_092100) might play a defensive role during the early stages of drug selection, similarly to *S. cerevisiae*, which protects itself from the toxin of *Kluyveromyces lactis* through its chitinase activity, possibly by binding to toxin or impairment of its uptake.[60] It was also reported that treatment of *Candida albicans* with chitinase resulted in increased resistance to amphotericin B.[61] The precise relationship of trifluoromethionine resistance and chitinase activity, however, remains to be demonstrated.

Several genes implicated in stress response were also modulated in TFMR. Glutamate synthase (EHI_045340; designated as NADPH-dependent oxidoreductase 2) belongs to the family of oxidoreductases, and in yeast its overexpression results in

resistance to methionine sulfoximine and tabtoxin.[62] In *E. histolytica* the enzyme plays an important role in redox maintenance, L-cysteine/L-cystine homeostasis, iron reduction and metronidazole activation.[63] Protein degradation mediated by Ulp1 (EHI_166820), on the other hand, is recognized to be critical in the regulation of the cell cycle, transcription and signal transduction.[64,65] Its upregulation indicates that a ubiquitin-dependent proteolysis pathway was activated in response to trifluoromethionine, and suggests involvement of the ubiquitin-proteasome system in drug resistance. The precise mechanism by which protein degradation may affect drug resistance remains to be determined. It is not clear how reduced proliferation occurs in the presence of these upregulated metabolic genes. It is likely that the effects of the repressed genes are more important and hence led to the reduced growth rate.

Two genes whose products bind nucleic acids were upregulated in TFMR. A zinc finger protein (EHI_176800) contains a DNA-binding domain and functions as part of transcription factor complex conferring DNA sequence specificity. In cancer cells resistant to anticancer drugs, its levels are increased, suggesting that it plays a role in cell survival.[66] Its overexpression in TFMR cells might be related to drug resistance, but identifying the relevant signalling mediators requires further investigation. DNA methyltransferase (EHI_121470), on the other hand, catalyses the transfer of a methyl group to DNA after replication, and epigenetically contributes to transcriptional regulation.[67] The increase in DNA methyltransferase expression in TFMR suggests that the differential expression of some of the proteins identified in this work is regulated by an epigenetic mechanism.

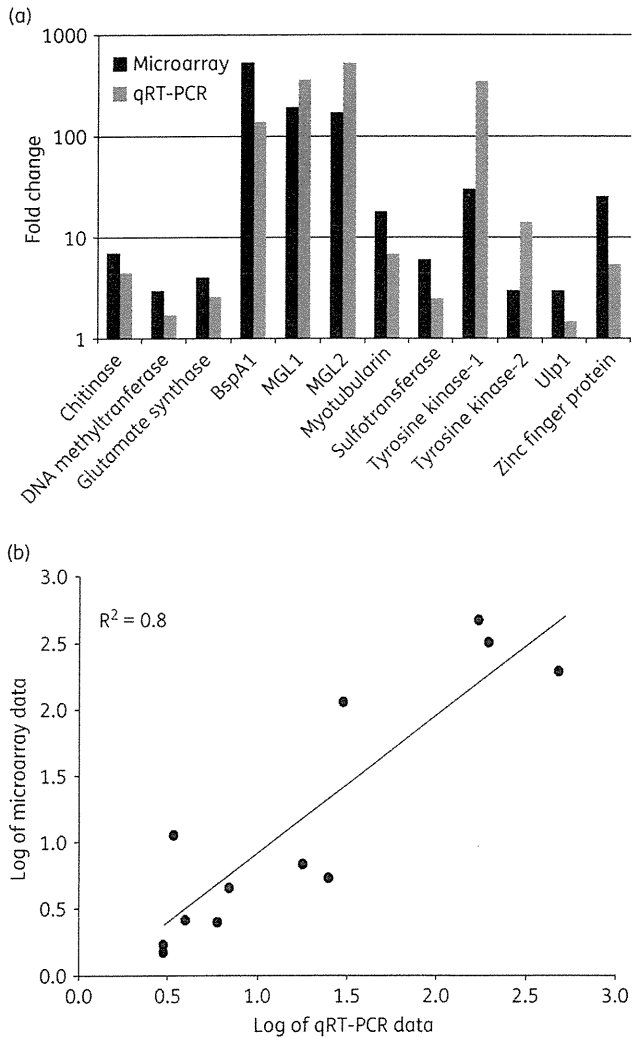

Figure 3. (a) Validation by qRT-PCR of microarray results for 12 differentially expressed genes. (b) Correlations between microarray and qRT-PCR fold changes of the selected genes indicate similar trend of gene expression ($R^2 = 0.8$).

Comparative transcriptome analysis

To determine whether the transcriptome profile we observed was specific for TFMR, we compared it to those of the strains specifically targeted to silence *EhMGL* genes (*Eh*MGL1gs and *Eh*MGL2gs), the strain selected for reduced susceptibility to 8 μM metronidazole (MTZR) and the strain grown under cysteine-deprived conditions for 24 h [Cys(−)] (Figure 2a). The results indicate that TFMR has a distinct signature profile (Figure 2b). Comparison between TFMR and *Eh*MGLgs showed that only *Eh*MGL1 and *Eh*MGL2 were commonly repressed in all three strains, except for a phosphatase domain-containing protein (EHI_085640), which was shared with *Eh*MGL2gs. While all three strains were resistant to trifluoromethionine, the small number of genes they have in common indicates that the mechanism by which *Eh*MGL repression occurred and the accompanying changes in gene expression, are clearly different between TFMR and *Eh*MGLgs. It was also particularly striking that the upregulation of *Eh*BspA1 occurred only in TFMR, confirming that it plays an important role in trifluoromethionine resistance.

Similarly, only four differentially expressed genes in TFMR were common to MTZR, and just two to Cys(−) (Figure 2b). It should be noted, however, that while the fold changes in the gene

Figure 4. (a) Upper panel: upregulation of *Eh*BspA1 expression in TFMR. cDNA was reverse transcribed from 5 μg of RNA and RT-PCR was performed with *Eh*BspA1-specific primers. Resolved products on 1.5% (*w/v*) agarose gel show that *Eh*BspA1 was not expressed in HM-1. Lower panel: total protein of *Eh*BspA1-HA and pEhEx-HA control transformants was separated on a 12% (*w/v*) SDS-polyacrylamide gel, electrotransferred onto nitrocellulose membranes, and reacted with anti-HA antibody. (b) Expression levels of *Eh*BspA1 in *Eh*BspA1-HA and pEhEx-HA were determined by qRT-PCR. (c) Immunofluorescence assay with anti-HA antibody indicates that *Eh*BspA1 is localized in the cytoplasm. Bar=10 μm. (d) Colorimetric determination of cells on coated plates shows no significant difference in adhesion between *Eh*BspA1-HA and the pEhEx-HA control. (e) Dose concentration-response curve of trifluoromethionine against *Eh*BspA1-HA overexpressing and pEhEx control strains. *Eh*BspA1-HA was partially resistant to trifluoromethionine with an IC_{50} of 25.1 μM compared with 13.8 μM in the pEhEx control. This figure appears in colour in the online version of *JAC* and in black and white in the printed version of *JAC*.

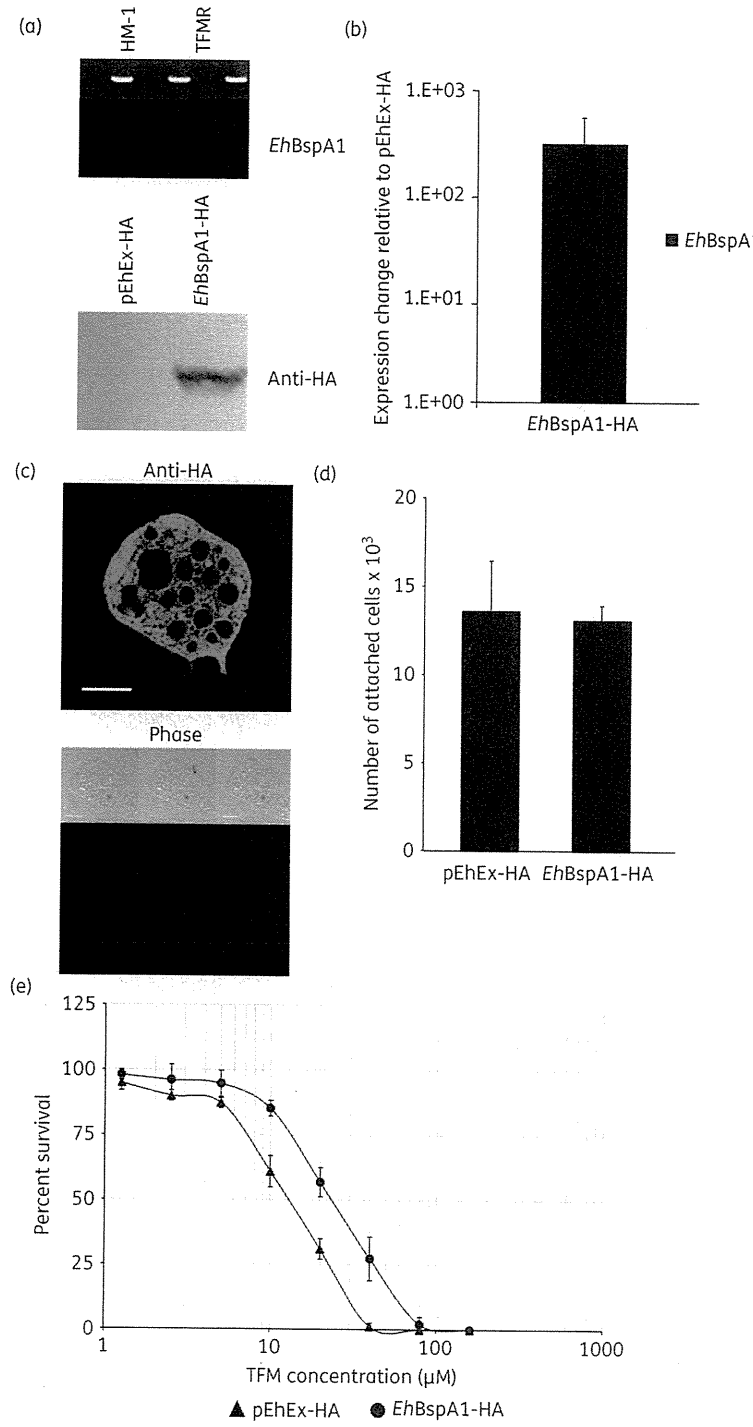

expression were comparable between the strains examined, their regulation was not always the same. Glutamate synthase (NADPH-dependent oxidoreductase) was upregulated in TFMR, while it was downregulated in MTZR and Cys(−). Downregulation of the enzyme in MTZR was expected because glutamate synthase has been implicated in the activation of metronidazole in *E. histolytica*.[63] The lack of significant overlap between modulated genes in TFMR and MTZR was not surprising because the mode of action of trifluoromethionine and metronidazole is different.[6–8,14–17] Previously we showed that TFMR is not cross-resistant to metronidazole.[19] Since MTZR only showed reduced susceptibility to metronidazole, it is unlikely that major mechanisms responsible for resistance were already established in the strain. TFMR and MTZR were therefore at different stages of resistance, but the modulated genes they have in common may play roles in stress response, which are often necessary in developing drug resistance. The specific regulation of genes in TFMR compared with Cys(−), on the other hand, indicates that the modulated genes in TFMR were not simply responses to stress but constitute a specific reaction towards developing resistance. Overall, differences in the profiles between strains illustrate that the transcriptional response of *E. histolytica* to trifluoromethionine is specific (Figure 2b) and could be used as a signature profile of trifluoromethionine resistance.

Conclusion

The use of a DNA microarray has provided a genome-wide analysis of trifluoromethionine resistance in *E. histolytica*. We have shown that drug resistance is both multifactorial and specific, involving not just the repression of *Eh*MGL, but the induction of *Eh*BspA1 and the differential expression of a host of genes involved in metabolism, stress response and gene regulation. While the exact relationship between these genes is largely unknown, it is likely that, *in vivo*, these are the same changes necessary to initiate, support and extend trifluoromethionine resistance. If proven to be true, it will then be possible to design a PCR-based test to detect trifluoromethionine resistance in the future, allowing for more suitable treatments and improving the clinical outcome of chemotherapy.

Acknowledgements

We thank Yumiko Saito-Nakano, Yuki Hanadate, Takashi Makiuchi and other members of our laboratory for technical assistance and valuable discussions.

Funding

This work was supported by a Grant-in-Aid for Scientific Research from the Ministry of Education, Culture, Sports, Science and Technology (MEXT) of Japan (18GS0314, 18050006, 18073001, 20390119, 23390099), a grant for research on emerging and re-emerging infectious diseases from the Ministry of Health, Labour and Welfare of Japan (H20-Shinkosaiko-ippan-016, H23-Shinkosaiko-ippan-014), a grant for research to promote the development of anti-AIDS pharmaceuticals from the Japan Health Sciences Foundation (KAA1551, KHA1101) and by Global COE Program (Global COE for Human Metabolomic Systems Biology) from MEXT, Japan.

Transparency declarations

None to declare.

Supplementary data

Tables S1–S5 and Figure S1 are available as Supplementary data at *JAC* Online (http://jac.oxfordjournals.org/).

References

1 Das MK, Lumb V, Mittra P *et al.* High chloroquine treatment failure rates and predominance of mutant genotypes associated with chloroquine and antifolate resistance among falciparum malaria patients from the island of Car Nicobar, India. *J Antimicrob Chemother* 2010; **65**: 1258–61.

2 Upcroft JA, Dunn LA, Wal T *et al.* Metronidazole resistance in *Trichomonas vaginalis* from highland women in Papua New Guinea. *Sex Health* 2009; **6**: 334–8.

3 Müller J, Sterk M, Hemphill A *et al.* Characterization of *Giardia lamblia* WB C6 clones resistant to nitazoxanide and to metronidazole. *J Antimicrob Chemother* 2007; **60**: 280–7.

4 Dunne RL, Dunn LA, Upcroft P *et al.* Drug resistance in the sexually transmitted protozoan *Trichomonas vaginalis*. *Cell Res* 2003; **13**: 239–49.

5 Vincent IM, Creek D, Watson DG *et al.* A molecular mechanism for eflornithine resistance in African trypanosomes. *PLoS Pathog* 2010; **6**: e1001204.

6 Wassmann C, Bruchhaus I. Superoxide dismutase reduces susceptibility to metronidazole of the pathogenic protozoan *Entamoeba histolytica* under microaerophilic but not under anaerobic conditions. *Arch Biochem Biophys* 2000; **376**: 236–8.

7 Wassmann C, Hellberg A, Tannich E *et al.* Metronidazole resistance in the protozoan parasite *Entamoeba histolytica* is associated with increased expression of iron-containing superoxide dismutase and peroxiredoxin and decreased expression of ferredoxin 1 and flavin reductase. *J Biol Chem* 1999; **274**: 26051–6.

8 Samarawickrema NA, Brown DM, Upcroft JA *et al.* Involvement of superoxide dismutase and pyruvate:ferredoxin oxidoreductase in mechanisms of metronidazole resistance in *Entamoeba histolytica*. *J Antimicrob Chemother* 1997; **40**: 833–40.

9 Ghosh SK, Lohia A, Kumar A *et al.* Overexpression of P-glycoprotein gene 1 by transfected *Entamoeba histolytica* confers emetine-resistance. *Mol Biochem Parasitol* 1996; **82**: 257–60.

10 Descoteaux S, Ayala P, Samuelson J *et al.* Increase in mRNA of multiple Eh pgp genes encoding P-glycoprotein homologues in emetine-resistant *Entamoeba histolytica* parasites. *Gene* 1995; **164**: 179–84.

11 Seydel KB, Stanley SL Jr. *Entamoeba histolytica* induces host cell death in amebic liver abscess by a non-Fas-dependent, non-tumor necrosis factor alpha-dependent pathway of apoptosis. *Infect Immun* 1998; **66**: 2980–3.

12 Martins A, Spengler G, Rodrigues L *et al.* pH Modulation of efflux pump activity of multi-drug resistant *Escherichia coli*: protection during its passage and eventual colonization of the colon. *PLoS One* 2009; **4**: e6656.

13 Löfmark S, Edlund C, Nord CE. Metronidazole is still the drug of choice for treatment of anaerobic infections. *Clin Infect Dis* 2010; **50**: S16–23.

14 Sato D, Kobayashi S, Yasui H *et al.* Cytotoxic effect of amide derivatives of trifluoromethionine against the enteric protozoan parasite *Entamoeba histolytica*. *Int J Antimicrob Agents* 2010; **35**: 56–61.

15 Sato D, Yamagata W, Harada S *et al.* Kinetic characterization of methionine γ-lyases from the enteric protozoan parasite *Entamoeba*

histolytica against physiological substrates and trifluoromethionine, a promising lead compound against amoebiasis. *FEBS J* 2008; **275**: 548–60.

16 Coombs GH, Mottram JC. Trifluoromethionine, a prodrug designed against methionine gamma-lyase-containing pathogens, has efficacy *in vitro* and *in vivo* against *Trichomonas vaginalis*. *Antimicrob Agents Chemother* 2001; **45**: 1743–5.

17 Alston TA, Bright HJ. Conversion of trifluoromethionine to a cross-linking agent by gamma-cystathionase. *Biochem Pharmacol* 1983; **32**: 947–50.

18 Zygmunt WA, Tavormina PA. DL-S-Trifluoromethylhomocysteine, a novel inhibitor of microbial growth. *Can J Microbiol* 1966; **12**: 143–8.

19 Penuliar GM, Furukawa A, Sato D *et al.* Mechanism of trifluoromethionine resistance in *Entamoeba histolytica*. *J Antimicrob Chemother* 2011; **66**: 2045–52.

20 Friedrich T, Rahmann S, Weigel W *et al.* High-throughput microarray technology in diagnostics of enterobacteria based on genome-wide probe selection and regression analysis. *BMC Genomics* 2010; **11**: 591.

21 Dharia NV, Bright AT, Westenberger SJ *et al.* Whole-genome sequencing and microarray analysis of *ex vivo Plasmodium vivax* reveal selective pressure on putative drug resistance genes. *Proc Natl Acad Sci USA* 2010; **107**: 20045–50.

22 Provvedi R, Palù G, Manganelli R. Use of DNA microarrays to study global patterns of gene expression. *Methods Mol Biol* 2009; **465**: 95–110.

23 Diamond LS, Harlow DR, Cunnick CC. A new medium for the axenic cultivation of *Entamoeba histolytica* and other *Entamoeba*. *Trans R Soc Trop Med Hyg* 1978; **72**: 431–2.

24 Husain A, Jeelani G, Sato D *et al.* Global Analysis of Gene Expression in Response to LCysteine Deprivation in the Anaerobic Protozoan Parasite *Entamoeba histolytica*. *BMC Genomics* 2011; **12**: 275.

25 GeneChip Expression Analysis Technical Manual. http://media.affymetrix.com/support/downloads/manuals/expression_analysis_technical_manual.pdf (28 September 2011, date last accessed).

26 Gilchrist CA, Houpt E, Trapaidze N *et al.* Impact of intestinal colonization and invasion on the *Entamoeba histolytica* transcriptome. *Mol Biochem Parasitol* 2006; **147**: 163–76.

27 GeneChip Expression Analysis: Data Analysis Fundamentals. http://media.affymetrix.com/support/downloads/manuals/data_analysis_fundamentals_manual.pdf (28 September 2011, date last accessed).

28 Altschul SF, Gish W, Miller W *et al.* Basic local alignment search tool. *J Mol Biol* 1990; **215**: 403–10.

29 Ehrenkaufer GM, Haque R, Hackney JA *et al.* Identification of developmentally regulated genes in *Entamoeba histolytica*: insights into mechanisms of stage conversion in a protozoan parasite. *Cell Microbiol* 2007; **9**: 1426–44.

30 Gene Ontology Annotation Database. http://www.ebi.ac.uk (28 September 2011, date last accessed).

31 Pathema-Entamoeba. http://pathema.jcvi.org/cgi-bin/Entamoeba/PathemaHomePage.cgi (28 September 2011, date last accessed).

32 HMMTOP—Prediction of transmembrane helices and topology of proteins. http://www.enzim.hu/hmmtop/ (28 September 2011, date last accessed).

33 SOSUI—Prediction of transmembrane regions. http://bp.nuap.nagoya-u.ac.jp/sosui/sosuiG/sosuigsubmit.html (28 September 2011, date last accessed).

34 TMHMM Server v. 2.0. Prediction of transmembrane helices in proteins. http://www.cbs.dtu.dk/services/TMHMM/ (28 September 2011, date last accessed).

35 TopPred 0.01: Topology prediction of membrane proteins. http://mobyle.pasteur.fr/cgi-bin/portal.py?#forms::toppred (28 September 2011, date last accessed).

36 TMpred—Prediction of Transmembrane Regions and Orientation. http://www.ch.embnet.org/software/TMPRED_form.html (28 September 2011, date last accessed).

37 Phobius. http://www.ebi.ac.uk/Tools/phobius/ (28 September 2011, date last accessed).

38 SignalP 3.0 Server. http://www.cbs.dtu.dk/services/SignalP/ (28 September 2011, date last accessed).

39 SOSUIsignal. http://bp.nuap.nagoya-u.ac.jp/sosui/sosuisignal/sosuisignal_submit.html (28 September 2011, date last accessed).

40 Heatmap Builder. http://ashleylab.stanford.edu/tools_scripts.html (28 September 2011, date last accessed).

41 Venn Diagram Generator. http://www.pangloss.com/seidel/Protocols/venn.cgi (28 September 2011, date last accessed).

42 Gene Expression Omnibus (GEO). http://www.ncbi.nlm.nih.gov/geo/ (28 September 2011, date last accessed).

43 Saito-Nakano Y, Yasuda T, Nakada-Tsukui K *et al.* Rab5-associated vacuoles play a unique role in phagocytosis of the enteric protozoan parasite *Entamoeba histolytica*. *J Biol Chem* 2004; **279**: 49497–507.

44 Nakada-Tsukui K, Okada H, Mitra BN *et al.* Phosphatidylinositol-phosphates mediate cytoskeletal reorganization during phagocytosis via a unique modular protein consisting of RhoGEF/DH and FYVE domains in the parasitic protozoon *Entamoeba histolytica*. *Cell Microbiol* 2009; **11**: 1471–91.

45 Nakada-Tsukui K, Saito-Nakano Y, Ali V *et al.* A retromerlike complex is a novel Rab7 effector that is involved in the transport of the virulence factor cysteine protease in the enteric protozoan parasite *Entamoeba histolytica*. *Mol Biol Cell* 2005; **16**: 5294–303.

46 Tanaka H, Esaki N, Soda K. A versatile bacterial enzyme: L-methionine γ-lyase. *Enzyme Microb Technol* 1985; **7**: 530–7.

47 Upcroft JA, Upcroft P. Keto-acid oxidoreductases in the anaerobic protozoa. *J Eukaryot Microbiol* 1999; **46**: 447–9.

48 Davis PH, Zhang Z, Chen M *et al.* Identification of a family of BspA like surface proteins of *Entamoeba histolytica* with novel leucine rich repeats. *Mol Biochem Parasitol* 2006; **145**: 111–6.

49 Inagaki S, Kuramitsu HK, Sharma A. Contact-dependent regulation of a *Tannerella forsythia* virulence factor, BspA, in biofilms. *FEMS Microbiol Lett* 2005; **249**: 291–6.

50 Ikegami A, Honma K, Sharma A *et al.* Multiple functions of the leucine-rich repeat protein LrrA of *Treponema denticola*. *Infect Immun* 2004; **72**: 4619–27.

51 Hirt RP, Harriman N, Kajava AV. A novel potential surface protein in *Trichomonas vaginalis* contains a leucine-rich repeat shared by micro-organisms from all three domains of life. *Mol Biochem Parasitol* 2002; **125**: 195–9.

52 Daher W, Pierce R, Khalife J. Census, molecular characterization and developmental expression of Leucine-Rich-Repeat proteins in *Plasmodium falciparum*. *Mol Biochem Parasitol* 2007; **155**: 161–6.

53 Kitagawa K, Abdulle R, Bansal PK *et al.* Requirement of Skp1-Bub1 interaction for kinetochore-mediated activation of the spindle checkpoint. *Mol Cell* 2003; **11**: 1201–13.

54 Barbey R, Baudouin-Cornu P, Lee TA *et al.* Inducible dissociation of SCF(Met30) ubiquitin ligase mediates a rapid transcriptional response to cadmium. *EMBO J* 2005; **24**: 521–32.

55 Seol JH, Shevchenko A, Shevchenko A *et al.* Skp1 forms multiple protein complexes, including RAVE, a regulator of V-ATPase assembly. *Nat Cell Biol* 2001; **3**: 384–91.

56 Hug V, Johnston D, Finders M *et al.* Use of growth-stimulatory hormones to improve the in vitro therapeutic index of doxorubicin for human breast tumors. *Cancer Res* 1986; **46**: 147–52.

57 Bishop AJ, Kosaras B, Carls N *et al.* Susceptibility of proliferating cells to benzo[a]pyrene-induced homologous recombination in mice. *Carcinogenesis* 2001; **22**: 641–9.

58 Klüppel M, Wight TN, Chan C *et al.* Maintenance of chondroitin sulfation balance by chondroitin-4-sulfotransferase 1 is required for chondrocyte development and growth factor signaling during cartilage morphogenesis. *Development* 2005; **132**: 3989–4003.

59 Shridhar V, Bible KC, Staub J *et al.* Loss of expression of a new member of the DNAJ protein family confers resistance to chemotherapeutic agents used in the treatment of ovarian cancer. *Cancer Res* 2001; **61**: 4258–65.

60 Gooday GW. Aggressive and defensive roles for Chitinases. In: Jolles P, Muzzarelli RA, eds. *Chitin and Chitinases*. Germany: Birkhauser Verlag, 1999; 157–69.

61 Bahmed K, Bonaly R, Coulon J. Relation between cell wall chitin content and susceptibility to amphotericin B in *Kluyveromyces, Candida* and *Schizosaccharomyces* species. *Res Microbiol* 2003; **154**: 215–22.

62 Marek ET, Dickson RC. Cloning and characterization of *Saccharomyces cerevisiae* genes that confer L-methionine sulfoximine and tabtoxin resistance. *J Bacteriol* 1987; **169**: 2440–8.

63 Jeelani G, Husain A, Sato D *et al.* Two atypical L-cysteine-regulated NADPH-dependent oxidoreductases involved in redox maintenance, L-cystine and iron reduction, and metronidazole activation in the enteric protozoan *Entamoeba histolytica*. *J Biol Chem* 2010; **285**: 26889–99.

64 Mossessova E, Lima CD. Ulp1-SUMO crystal structure and genetic analysis reveal conserved interactions and a regulatory element essential for cell growth in yeast. *Mol Cell* 2000; **5**: 865–76.

65 Chosed R, Mukherjee S, Lois LM *et al.* Evolution of a signalling system that incorporates both redundancy and diversity: Arabidopsis SUMOylation. *Biochem J* 2006; **398**: 521–9.

66 Paek AR, Kim SH, Kim SS *et al.* IGF-1 induces expression of zinc-finger protein 143 in colon cancer cells through phosphatidylinositide 3-kinase and reactive oxygen species. *Exp Mol Med* 2010; **42**: 696–702.

67 Razin A, Cedar H. DNA methylation and gene expression. *Microbiol Rev* 1991; **55**: 451–8.

Novel Transmembrane Receptor Involved in Phagosome Transport of Lysozymes and β-Hexosaminidase in the Enteric Protozoan *Entamoeba histolytica*

Atsushi Furukawa[1,2], Kumiko Nakada-Tsukui[1], Tomoyoshi Nozaki[1,3]*

1 Department of Parasitology, National Institute of Infectious Diseases, Toyama, Shinjuku-ku, Tokyo, Japan, **2** Department of Parasitology, Gunma University Graduate School of Medicine, Showa-machi, Maebashi, Japan, **3** Graduate School of Life and Environmental Sciences, University of Tsukuba, Tennoudai, Tsukuba, Ibaraki, Japan

Abstract

Lysozymes and hexosaminidases are ubiquitous hydrolases in bacteria and eukaryotes. In phagocytic lower eukaryotes and professional phagocytes from higher eukaryotes, they are involved in the degradation of ingested bacteria in phagosomes. In *Entamoeba histolytica*, which is the intestinal protozoan parasite that causes amoebiasis, phagocytosis plays a pivotal role in the nutrient acquisition and the evasion from the host defense systems. While the content of phagosomes and biochemical and physiological roles of the major phagosomal proteins have been established in *E. histolytica*, the mechanisms of trafficking of these phagosomal proteins, in general, remain largely unknown. In this study, we identified and characterized for the first time the putative receptor/carrier involved in the transport of the above-mentioned hydrolases to phagosomes. We have shown that the receptor, designated as cysteine protease binding protein family 8 (CPBF8), is localized in lysosomes and mediates transport of lysozymes and β-hexosaminidase α-subunit to phagosomes when the amoeba ingests mammalian cells or Gram-positive bacillus *Clostridium perfringens*. We have also shown that the binding of CPBF8 to the cargos is mediated by the serine-rich domain, more specifically three serine residues of the domain, which likely contains trifluoroacetic acid-sensitive O-phosphodiester-linked glycan modifications, of CPBF8. We further showed that the repression of CPBF8 by gene silencing reduced the lysozyme and β-hexosaminidase activity in phagosomes and delayed the degradation of *C. perfringens*. Repression of CPBF8 also resulted in decrease in the cytopathy against the mammalian cells, suggesting that CPBF8 may also be involved in, besides the degradation of ingested bacteria, the pathogenesis against the mammalian hosts. This work represents the first case of the identification of a transport receptor of hydrolytic enzymes responsible for the degradation of microorganisms in phagosomes.

Citation: Furukawa A, Nakada-Tsukui K, Nozaki T (2012) Novel Transmembrane Receptor Involved in Phagosome Transport of Lysozymes and β-Hexosaminidase in the Enteric Protozoan *Entamoeba histolytica*. PLoS Pathog 8(2): e1002539. doi:10.1371/journal.ppat.1002539

Editor: Patricia J. Johnson, University of California Los Angeles, United States of America

Received August 15, 2011; **Accepted** January 5, 2012; **Published** February 23, 2012

Funding: This work was supported by a Grant-in-Aid for Scientific Research from the Ministry of Education, Culture, Sports, Science and Technology (MEXT) of Japan (18GS0314, 18050006, 18073001, 20390119, 23390099) and to K.N-T. (18790291, 20790323), a grant for research on emerging and re-emerging infectious diseases from the Ministry of Health, Labour and Welfare of Japan (H20-Shinko-ippan-016, H23-Shinko-ippan-014), a grant for research to promote the development of anti-AIDS pharmaceuticals from the Japan Health Sciences Foundation (KAA1551, KHA1101), and by Global COE Program (Global COE for Human Metabolomic Systems Biology) from MEXT, Japan. The funders had no role in study design, data collection and analysis, decision to publish, or preparation of the manuscript.

Competing Interests: The authors have declared that no competing interests exist.

* E-mail: nozaki@nih.go.jp

Introduction

Lysozymes (EC 3.2.1.17) are the antibacterial protein that has an ability to damage the cell wall of bacteria [1]. The enzyme acts by catalyzing the hydrolysis of 1,4-beta-linkages between *N*-acetylmuramic acid and *N*-acetyl-D-glucosamine in peptidoglycans and between the *N*-acetyl-D-glucosamine residues in chitodextrins. While biochemical [2], functional [3], and structural [4] features of lysozymes have been well established, the mechanisms for intracellular trafficking and secretion remain poorly characterized except for the report that showed that condroitin sulfate is involved in lysosomal targeting of lysozymes [5]. Hexosaminidase (EC 3.2.1.52) is involved in the hydrolysis of terminal N-acetyl-D-hexosamine residues in hexosaminides. Three dimeric isozymes of β-hexosaminidase are formed by the combination of α and β subunits, encoded by *HEXA* and *HEXB* genes, respectively. β-Hexosaminidase and the cofactor GM2 activator protein catalyze the degradation of the GM2 gangliosides containing terminal N-acetyl hexosamines [6]. Mutations in *HEXA* gene decrease the hydrolysis of GM2 gangliosides, which is the main cause of Tay-Sachs disease, whereas mutations in *HEXB* gene results in Sandhoff disease [7]. The trafficking mechanism of β-hexosaminidase via mannose-6-phosphate receptor has been well studied in mouse lymphoma and myeloma cell [8–10]. However, the mechanisms of trafficking of β-hexosaminidase in eukaryotes besides mammals remain to be discovered.

Lysozyme and β-hexosaminidase are abundant components found in phagosomes from *Entamoeba histolytica* [11,12], which is the anaerobic or microaerophilic protozoan parasite, causing amebic dysentery and amebic liver abscesses in an estimated 10 million cases annually [13]. However, the role and intracellular trafficking of these enzymes remain unknown. Phagocytosis and phagosome biogenesis seems to play a pivotal role in pathogenesis in *E. histolytica* [14]. *E. histolytica* is capable of internalizing

Author Summary

Phagocytosis is the cellular process of engulfing solid particles to form an internal phagosome in protozoa, algae, and professional phagocytes of multicellular eukaryotic organisms. In phagocytic protozoa, phagocytosis is involved in the acquisition of nutrients, and the evasion from the host immune system and inflammation. While hydrolytic enzymes that are essential for the efficient and regulated degradation of phagocytosed particles, such as bacteria, fungi, and eukaryotic organisms, have been characterized, the mechanisms of the transport of these proteins are poorly understood. In the present study, we have demonstrated, for the first time, the molecular mechanisms of how the digestive enzymes are transported to phagosomes. Understanding of such mechanisms of the transport of phagosomal proteins at the molecular level may lead to the identification of a novel target for the development of new preventive measures against parasitic infections caused by phagocytic protozoa.

extracellular particles by phagocytosis. The amebic trophozoites ingest microorganisms in the large intestine [15,16], and host cells including non-immune cells [17], and immune cells [18] during tissue invasion. It has been well-established that in vitro and in vivo virulence correlates well with the ability of phagocytosis [14,19,20]. Furthermore, phagosomes contain a panel of proteins that were shown to be crucial in pathogenesis such as cysteine proteases (CPs) [21], amoeba pores [22], and galactose/N-acetylgalactosamine-specific lectin [23,24], proteins involved in cytoskeletal reorganization [25,26], vesicular trafficking [27–29], and signal transduction [30,31]. Therefore, understanding the molecular mechanisms of phagocytosis and phagosome biogenesis as well as the role and trafficking of individual phagosomal proteins in phagosomes, should help to understand underlying links between phagocytosis and pathogenicity.

Recently, the proteins and mechanisms involved in phagocytosis have been demonstrated. For instance, the surface Ca^{2+}-binding kinase (C2PK) has shown to be involved in the initiation of phagocytosis [31]. The antisense inhibition of C2PK caused inhibition of the initiation of erythrophagocytosis. It has also been shown that surface transmembrane kinase (TMK96) and p21-activated kinase (PAK) play an important role in phagocytosis of human erythrocytes [32,33]. The unconventional myosin, myosin IB, was shown to be involved in cytoskeleton rearrangement during phagocytosis [25,26]. Furthermore, phosphatidylinositides also play critical roles during phagocytosis [34,35]. Our previous proteomic studies, where 159 proteins were identified from purified phagosomes [11,12], also suggested a direct link between phagosome biogenesis and pathogenesis, as phagosomes contained a panel of proteins that were shown to be crucial in pathogenesis described above. Furthermore, the proteins that are implicated for degradation of phagocytosed bacteria, e.g. amoebapores [22], lysozymes, and β-hexosaminidase, as well as other hydrolytic enzymes such as amylase and ribonuclease were also demonstrated in phagosomes. While both the constituents of phagosomes and the kinetics of their recruitment are known, very little is known on how these proteins are transported to phagosomes. Recently, we discovered a putative transmembrane receptor for cysteine proteases from *E. histolytica*, which preferentially binds to CP5 (Nakada-Tsukui K, et al., unpublished data), which is directly implicated in the pathogenesis [36–38]. The *E. histolytica* genome contained a total of 11 members showing significant mutual identity and structural conservation to the transmembrane cysteine protease receptor: the signal peptide at the amino terminus, a single transmembrane domain close to the carboxyl terminus, and the YxxΦ motif at the carboxyl terminus. This family of proteins was designated as cysteine protease binding family proteins 1–11 (CPBF1-11). In the present study, we characterized one of the most highly expressed CPBF genes among the family, *CPBF8*. We showed that CPBF8 localizes to phagosomes during phagocytosis, while it is distributed to the acidic compartment in steady state. Affinity immunoprecipitation followed by LC-MS/MS analysis showed that CPBF8 specifically bound to lysozymes and β-hexosaminidase α-subunit. Repression of CPBF8 by gene silencing reduced lysozyme and β-hexosaminidase activities in phagosomes, and caused a defect of digestion of ingested bacteria.

Results

Localization of CPBF8

We examined the localization of CPBF8 during phagocytosis of CHO cells. Trophozoites of CPBF8-HA-expressing strain were incubated with CellTracker-loaded CHO cells for 10 to 60 min to allow ingestion of CHO cells. Immunofluorescence assay using anti-HA antibody showed that CPBF8 was localized to phagosomes containing CHO cells at all time points (10, 30, and 60 mins) (Figure 1A). CPBF8 remained associated with phagosomes in the course of phagocytosis: the percentage of colocalization did not significantly changed (84, 92 and 82% at 10, 30, and 60 min, respectively). Immunofluorescence image of the amoeba undergoing engulfment revealed that CPBF8 localized to the basolateral portion of a phagosome, and excluded from the tunnel-like structure connecting a phagosome and the CHO cell being aspirated [35].

As immunofluorescence assay showed that CPBF8 was also distributed to a large number of vesicles and vacuoles under quiescent (i.e., non-phagocytic) conditions, we examined the nature of these compartments. CPBF8-HA was associated with the acidic organelles labeled with membrane-diffusible LysoTracker under steady-state conditions (60% of LysoTracker-positive vesicles/vacuoles was positive for CPBF8) (Figure 1B). CPBF8 colocalized nicely with a vacuolar membrane protein, pyridine nucleotide transhydrogenase, *Eh*PNT, which converts NADPH and NADH using the proton gradient across the membrane [39] (Figure 1C). It has been shown that *Eh*PNT is localized to the acidic compartment in steady state and transported to phagosomes upon phagocytosis [40].

CPBF8 binds to β-hexosaminidase α-subunit and lysozymes

To identify potential cargo proteins that CPBF8 binds and carries to phagosomes, we immunoprecipitated proteins that bind to CPBF8, from the lysates of the transformant where HA-tagged CPBF8 was ectopically expressed (Figure 2). Silver stained SDS-PAGE gel revealed three major bands of about >120, 60, and 20 kDa (bands C, E, and F) and three minor bands of about >300, >200, and 75 kDa (bands A, B, and D) exclusively found in the immunoprecipitated sample from CPBF8-HA strain, but not from HA control strain. These bands were excised and subjected to LC-MS/MS analysis (Table 1 and Table S1). Smeary band C, which showed an apparent molecular mass of ~130 kDa on SDS-PAGE was identified as CPBF8 itself; the apparent size was larger than the predicted size (99.3 kDa), suggestive of post-translational modifications or aberrant structure (see below). Band E was identified as β-hexosaminidase α-subunit (XP_657529; EHI_148130) with 19.7% coverage. Band F was identified as a mixture

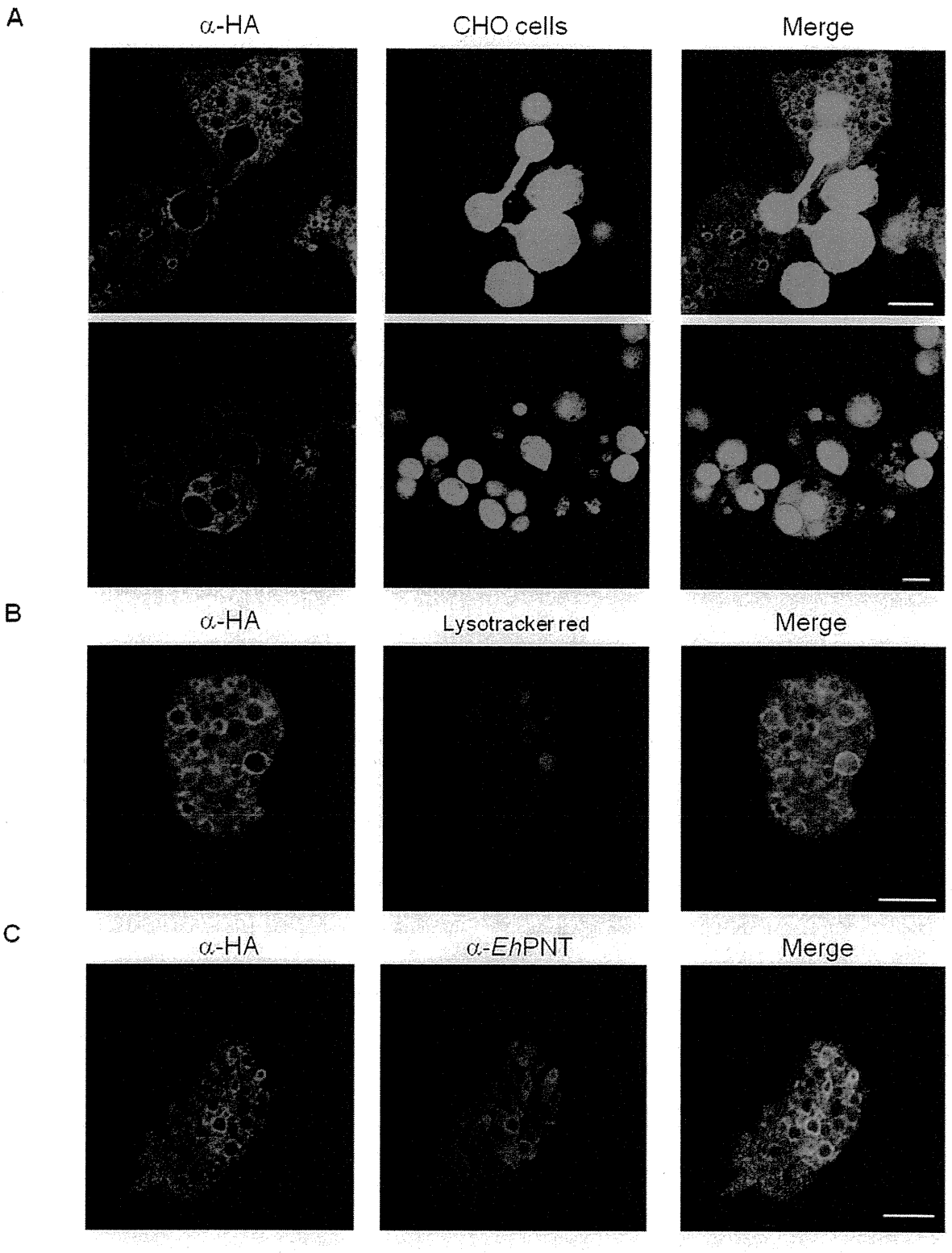

Figure 1. Localization of CPBF8 in *E. histolytica*. (A) Phagosome localization of CPBF8. Amoebae were incubated with Cell Tracker Blue-stained CHO cells (*blue*) for 10 (top row) or 60 minutes (bottom row), fixed, and reacted with anti-HA antibody (*green*). *Bar*, 10 μm. (B) Lysosomes localization of CPBF8. Amoebae were labeled with LysoTracker Red (*red*) and subjected to immunofluorescence assay with anti-HA antibody (*green*). Bar, 10 μm. (C) Colocalization of *Eh*PNT and CPBF8. The cells were fixed, and reacted with anti-*Eh*PNT (*red*) and anti-HA antibody (*green*). Bar, 10 μm.
doi:10.1371/journal.ppat.1002539.g001

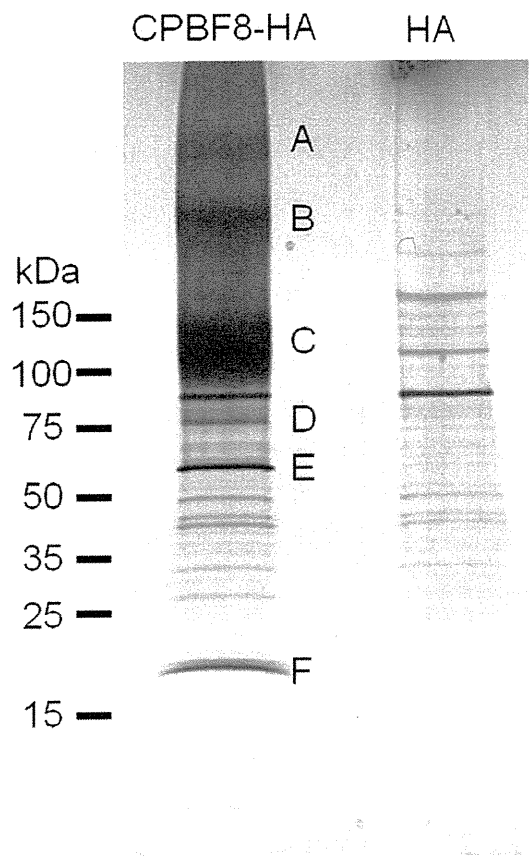

Figure 2. Isolation and identification of CPBF8-binding proteins. Lysates of CPBF8-HA and control ("HA") transformants were mixed with anti-HA-antibody-conjugated agarose, washed, and eluted with HA peptide. Immunoprecipitated samples were separated on SDS-PAGE and silver stained. Apparent molecular weight of standards (kDa) are indicated on the left. Six bands excised for protein identification are marked (A–F).
doi:10.1371/journal.ppat.1002539.g002

of lysozyme 1 (XP_653294, EHI_199110) and lysozyme 2 (XP_656933; EHI_096570) with 22.7 and 30.2% coverage, respectively. Lysozyme 1 and 2 were previously demonstrated by our previous phagosome proteome analysis [11,12]. Bands A, B, and D mostly corresponded to CPBF8 (Table S1). These data clearly indicate that β-hexosaminidase α-subunit and lysozymes are predominant proteins that bind CPBF8. β-hexosaminidase α-subunit was not previously detected by phagosome proteomics, whereas its β-subunit was detected.

Repression of CPBF8 by gene silencing decreases β-hexosaminidase and lysozyme activity

To further demonstrate the role of CPBF8, we created a strain in which CPBF8 expession was repressed by long term transcriptional gene silencing [41] ("CPBF8gs strain"). Gene silencing is mediated by nuclear localized antisense small RNAs with 5′-polyphosphate termini [42], and observed only in G3 and its derived strains, in which amoebapore genes have been repressed. RT-PCR analysis showed that the mRNA level of *CPBF8* gene in CPBF8gs strain was specifically reduced to the undetectable level (Figure 3A). DNA microarray analysis further verified that CPBF8 transcript was reduced by 326 fold, while the expression of other CPBF genes remained unchanged (Figure 3B). In *in vitro* cultivation CPBF8gs strain did not show any defect in growth compared to control pSAP2-Gunma-transfected strain (Supplemental information Figure S1). The doubling times of control and CPBF8gs strains were comparable (20.9 and 20.6 h, respectively). Thus, the defects in protein transport and the decrease in cytopathy against mammalian cells and bacteria digestion, described below, are not likely attributable to poor proliferation (growth) of CPBF8gs strain.

We examined β-hexosaminidase and lysozyme activities in CPBF8gs and control strains using a synthetic N-acetylglucosamine-related substrate (4-methylumbelliferyl-2-acetamido-2-deoxy-β-D-glucopyranoside, MUG) and its sulfo derivative (MUGS) (for β-hexosaminidase), and Bodipy-conjugated *Micrococcus lysodeikticus* cell wall (for lysozymes). The enzyme activity toward MUGS in the whole cells of CPBF8gs strain (0.045 U/g) decreased by 81%, compared to control (0.234) (Figure 4A), whereas that toward MUG reduced by 32% (44.4 and 30.4 U/g in control and CPBF8gs strain, respectively) (Figure 4B). The activity toward MUGS or MUG is known to attributable to β-hexosaminidase activity of a homodimer of α-subunit, or that of both a homodimer of β-subunit and a α/β-subunit heterodimer [43]. The β-hexosaminidase activity toward MUGS and MUG, secreted to the culture medium, also decreased by 37 and 43% in CPBF8gs strain, respectively. The lysozyme activities in the whole cell lysates of CPBF8gs strain appear to be slightly decreased (4.3%), while the amylase activity remained unchanged (Figures 4, C and D). One should know that the degree of lysozyme secretion was much higher than that of β-hexosaminidase. β-Hexosaminidase activity detected in the culture supernatant was almost negligible (Figure 4A and B), and may be attributable to lysed cells. In addition, lysozyme activity detected in the whole lysates and the culture supernatant appear to be attributable to proteins other than lysozyme 1 and 2 because the lysozyme activity in the isolated phagosomes and the amount of lysozyme 2 in the whole cells and

Table 1. Identification of CPBF-binding proteins by LC-MS/MS analysis.

Size of excised band (kDa) (name)	ID number of identified protein (GenBank ID)	Coverage (%)[1]	Annotation	Predicted molecular weight (kDa)
100–150 (C)	EHI_059830 (XM_647807)	35.1	CPBF8	99.3
60 (E)	EHI_148130 (XM_652437)	19.7	β-hexosaminidase α-subunit	61.0
20 (F)	EHI_199110 (XM_648202)	22.7	lysozyme	23.5
	EHI_096570 (XM_651841)	30.2	lysozyme	23.4

[1]coverage based on the peptides over 95% probability.
doi:10.1371/journal.ppat.1002539.t001

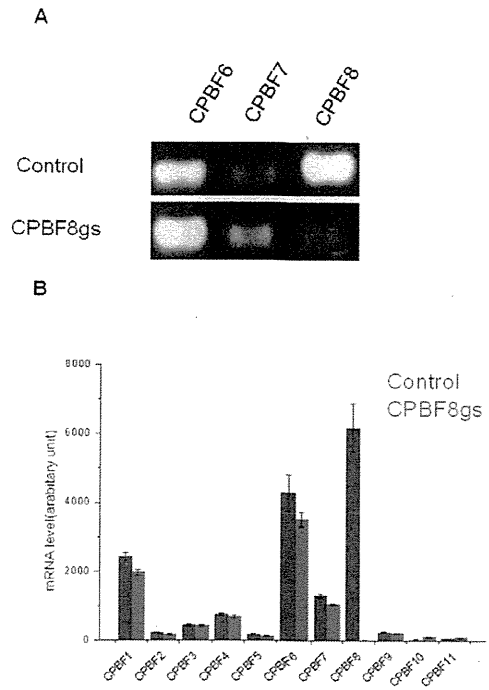

Figure 3. Specific repression of CPBF8 gene in CPBF8gs strain. (A) RT-PCR analysis. A 200 bp long partial *CPBF8* gene was amplified using cDNA from control and CPBF8gs strains. (B) DNA microarray analysis of CPBF genes (CPBF1-11). The raw fluorescence data of triplicates is shown.
doi:10.1371/journal.ppat.1002539.g003

phagosomes detected by specific antibody in immunoblot analysis greatly decreased (see below).

Phagosome targeting of β-hexosaminidase and lysozymes is inhibited by the repression of CPBF8

In order to further investigate whether CPBF8 is involved in trafficking of β-hexosaminidase α-subunit and lysozymes to phagosomes, we compared these activities in phagosomes isolated and purified, as previously described [12], from CPBF8gs and control strains (Figure 4E). We observed that β-hexosaminidase α-subunit and lysozyme activities in purified phagosomes decreased by 90 and 96%, respectively, in CPBF8gs, compared to the control strain, while the amylase activity in phagosomes remained unchanged. Immuno blot analysis also confirmed the results of the activity assays, and indicated that lysozyme 2 is not transported to phagosomes in CPBF8gs strain (Figure 4F).

Repression of CPBF8 inhibits digestion of ingested bacteria

To understand biological significance of CPBF8, we examined phagocytosis and degradation of a representative Gram-positive bacillus *Clostridium perfringens* in CPBF8gs strain. We microscopically monitored a course of degradation of ingested *C. perfringens* (Figure 5A). Intact and rod-shaped *C. perfringens* becomes rounded in phagosomes when it is permeabilized and degraded. After 4 h co-incubation of SYTO-59-prestained bacteria with the amoebae, both the rod-shaped and rounded bacteria were counted (Figure 5B). While the total number of bacteria ingested were comparable in the control and CPBF8gs strains (12.2±3.8 and 9.1±3.8 per amoeba, respectively), the number of rounded bacteria (0.3±0.4 per amoeba) dramatically decreased in CPBF8gs compared to the control (8.1±4.1 per amoeba), whereas that of rod-shaped bacteria increased by two fold (8.8±3.9 and 4.0±3.2, respectively). These results clearly indicate that degradation of *C. perfringens* was inhibited by the repression of CPBF8.

Repression of CPBF8 decreases the cytopathic activity

We investigated whether CPBF8 is involved in the cytopathic effects on monolayers of cultured mammalian cells. The monolayers of Chinese hamster ovary (CHO) cells were incubated with the control and CPBF8gs strains for 1–3 h, and destruction of CHO cells was measured. The cytopathic activity caused by CPBF8gs strain was lower by 23–29% at all time points compared to control strain (Figure 5C). The observed cytopathic effect was partially blocked by 200 μM of the cysteine protease inhibitor E-64 [44,45]. The cytopathic effect by the control strain was reduced by 20–22%, whereas that by CPBF8gs was decreased by 41–45% (Figure 5D). These results support the hypothesis that the decrease in the cytopathic activity in CPBF8gs was due to the decrease in β-hexosaminidase α-subunit and lysozymes.

To confirm this hypothesis, we also created the strains where β-hexosaminidase α-subunit or lysozyme 1 genes was repressed (HexAgs and Lys1gs strains). These silenced strains showed reduced cytotoxity to CHO cells compared to the control mock transformant by 9–18% reduction, as measured at 60 mins of co-incubation (Supplemental information Figure S2). These data indicate that secreted (and maybe also intracellular) lysozymes are involved in CHO cytolysis, and that intracellular β-hexosaminidase α-subunit is also involved in pathogenesis against mammalian cells, though its mechanism remains undetermined. We also attempted to directly test cytotoxic activity of recombinant hexosaminidase and lysozymes produced by in vitro translation (up to 10 μg/ml final), but failed to demonstrate it.

The serine-rich region in CPBF8 is responsible for the binding with its cargo, but not its localization

CPBF family proteins show common structural organization: the signal peptide at the amino terminus, the transmembrane domain close to the carboxyl-terminal end, and the YxxL motif in the cytosolic tail located at the carboxyl terminus (Nakada-Tsukui K, et al., unpublished data). Besides, among 11 members, only 3 members, CPBF6, CPBF7, and CPBF8, have a stretch of serine-rich hydrophilic region prior to the transmembrane domain (Figure 6A and B). In order to investigate whether this region is involved in the binding of CPBF8 to the cargos and whether the region is involved in the phagosomal transport, we created a transformant that expressed HA-tagged CPBF8 lacking the 23-a.a.-long serine-rich region (CPBF8ΔSRR-HA). We immunoprecipitated CPBF8-HA and CPBF8ΔSRR-HA using anti-HA antibody from lysates of the corresponding strains. Both the silver-stained SDS-PAGE gel and immunoblot analysis with HA antibody showed that the size of CPBF8ΔSRR-HA (~100 kDa) detected was ~50 kDa smaller than that of CPBF8-HA (~150 kDa), which was larger than predicted (Figure 6 E and F, see below *"The nature of post-translational modifications of CPBF8"*). The amount of the 75- and 25-kDa proteins, which correspond to β-hexosaminidase α-subunit and lysozymes, respectively, detected in the immunoprecipitated samples from the lysates of CPBF8ΔSRR-HA significantly decreased, compared to that from CPBF8-HA strain (Figure 6E and F). The identity of the precipitated proteins was confirmed by the immunoblots using anti-β-hexosaminidase α-subunit antibody and lysozyme 2 antibody (Figure 6F).

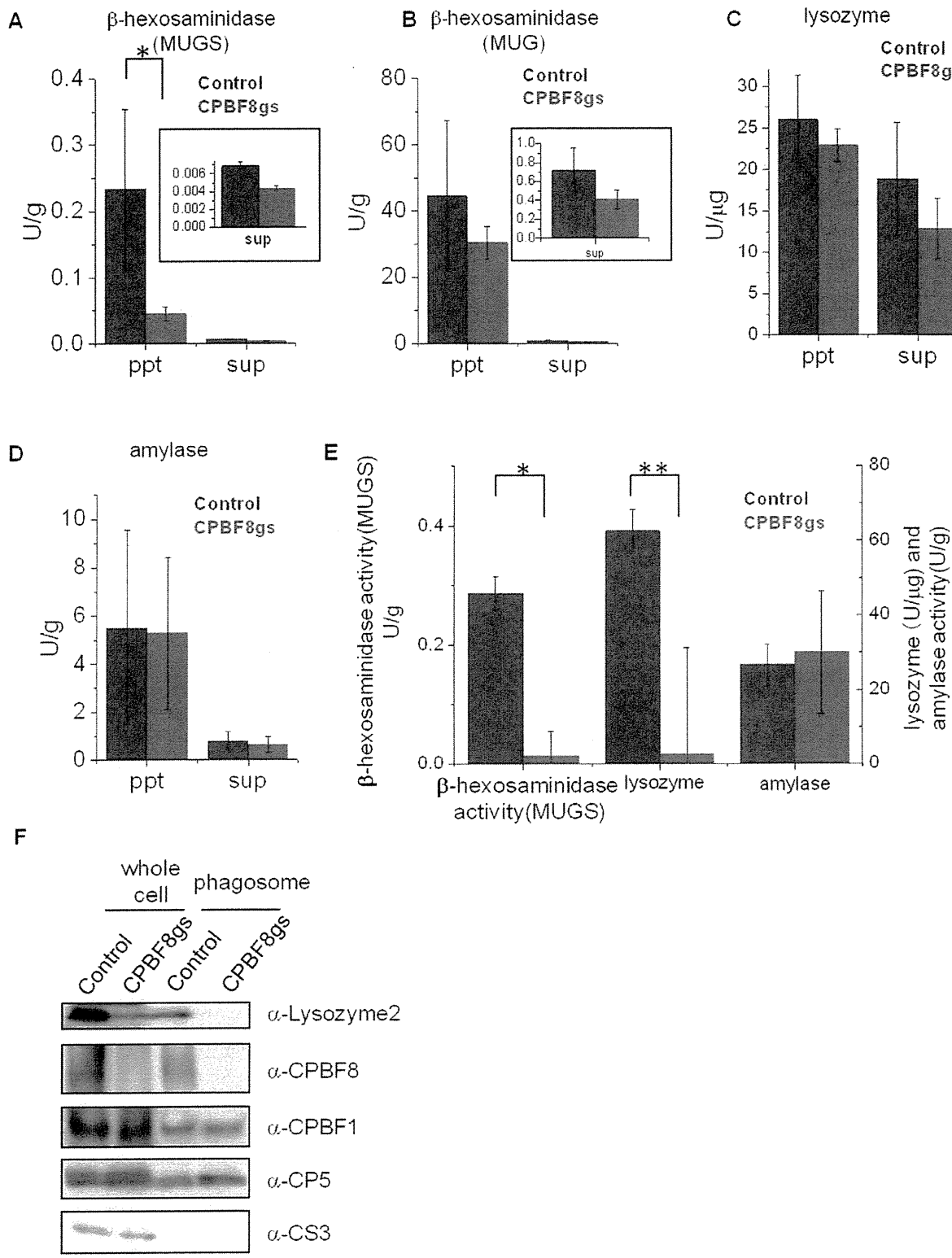

Figure 4. Enzymatic activities in total lysates, culture supernatant, and phagosomes and immuno blot analysis of total lysates and phagosomes derived from control and CPBF8gs strains. After the amoebas were incubated in fresh medium for 2 h, trophozoites and culture supernatant were separated by brief centrifugation. After the supernatant was removed ("sup"), the cell pellet was resuspended and solublized in lysis buffer ("ppt"). To isolate phagosomes (E), the amoebas were incubated with latex beads, and, after brief centrifugation, the cell pellet was

resuspended, and mechanically homogenized. The phagosomes were isolated by ultracentrifugation on a sucrose gradient. Enzymatic activities of culture supernatant, whole lysate (A–D), and phagosomes (E) are shown. (A–D) Enzymatic activities of β-hexosaminidase activity toward MUGS (A) and MUG (B), lysozyme activity (C), and amylase activity (D) in the cell pellet and culture supernatant. (E) Enzymatic activities of β-hexosaminidase toward MUGS, lysozyme, and amylase in phagosomes. Data shown are the means ± standard deviations of three independent experiments. "*" or "**" represents statistical significance at $p<0.01$ or $p<0.05$, respectively. (F) Immuno blot analysis of the cell pellet and the phagosome fraction. Approximately 20 μg of the cell pellet and 2 μg of the phagosome fraction were electrophoresed. CPBF1 and CP5 are phagosomal proteins, while cysteine synthase 3 (CS3) is a cytosolic marker. Abbreviations are: ppt, pellet fraction; sup, culture supernatant; phagosome, phagosome fraction.
doi:10.1371/journal.ppat.1002539.g004

To further map the region and amino acids responsible for the cargo binding, we constructed the variant forms of CPBF8 in which one of two stretches of three serines in the SRR were replaced by alanines (CPBF8AAA1-HA and CPBF8AAA2-HA, respectively) (Figure 6C). CPBF8AAA1-HA showed reduced ability to bind β-hexosaminidase α-subunit and lysozyme 2, compared to CPBF8-HA and CPBF8AAA2-HA (Figure 6E and F). These data indicate that the region containing the first stretch of three serine residues is essential for the binding with the cargos. Furthermore, silver staining and immunoblots with anti-HA antibody of the lysate from CPBF8AAA1-HA showed a ~20 kDa reduction in the apparent molecular size of CPBF8AAA1-HA, compared to CPBF8-HA. These data were also consistent with a premise that this portion is directly post-translationally modified or indirectly involved in post-translational modifications (see below). We also attempted to show direct evidence that β-hexosaminidase α-subunit and lysozymes bind to SRR by constructing a truncated form of CPBF8, in which the signal peptide, SRR, the transmembrane domain, and the cytosolic region of CPBF8 were included (designated as SRR-HA). However, neither β-hexosaminidase α-subunit nor lysozymes was detected by immunoprecipitation of SRR-HA (data not shown). This indicates that the SRR per se may not be sufficient for post-translational modifications required for cargo binding. Immunofluorescence assay showed that the localization of CPBF8ΔSRR-HA, CPBF8AAA1-HA, CPBF8 AAA2-HA, and SRR-HA such as phagosome recruitment (Figure 6D and Supplemental information Figure S3A–C) was indistinguishable from that of CPBF8-HA. Therefore, SRR does not appear to be essential to phagosome targeting.

The nature of post-translational modifications of CPBF8

The apparent molecular mass of CPBF8ΔSRR-HA detected with silver staining and immunoblots with anti-HA antibody was ~50 kDa smaller than that of CPBF8-HA (Figure 6, E and F, Figure 7). The reduction of the apparent size was larger than the predicted decrease based on the deletion of the amino acids (23 a.a. corresponding to 2.4 kDa for CPBF8ΔSRR-HA). To better understand the nature of the post-translational modification of CPBF8, we treated the transformant with 10 μg/ml tunicamycin, which is an inhibitor of asparagine-linked glycan modification, for 24 h (40). However, tunicamycin treatment did not affect the apparent mobility of immunoprecipitated CPBF8-HA on SDS-PAGE (data not shown), despite the fact that a potential N-linked glycosylation site is present in CPBF8 (Asn383). It was previously shown that the major GPI-anchored surface antigen of *E. histolytica* trophozoites contains O-phosphodiester-linked sugars [46]. We examined if the post-translational modification of CPBF8 contains O-phosphodiester-linked sugars by the treatment of immunoprecipitated CPBF8 with trifluoroacetic acid (TFA). SDS-PAGE and immunoblot analyses showed that TFM treatment of immunoprecipitated CPBF8 reduced the apparent molecular size of CPBF8 to ~120 kDa (Figure 7), which was similar to the size of CPBF8AAA1-HA (Figure 6, E and F), while that of CPBF8ΔSRR-HA remained unchanged by TFA treatment. Altogether, CPBF8 appears to possess O-phosphodiester linked carbohydrates via the first stretch of serines within SRR, and this region seems to be responsible for the binding with β-hexosaminidase α-subunit and lysozymes. It should also be noted that the apparent size of TFA-treated CPBF8-HA and CPBF8AAA1-HA was significantly (~20 kDa) larger than that of CPBF8ΔSRR-HA. The difference between CPBF8AAA1-HA and CPBF8ΔSRR-HA was apparently larger than the predicted size of SRR (2.4 kDa), suggesting that other post-translational modification(s) may be present in other region(s) of SRR.

Discussion

Discovery of a novel transport receptor of β-hexosaminidase α-subunit and lysozymes

CPBF8 was first identified in phagosomes by our previous proteome study of the purified phagosomes [12]. We have recently rediscovered CPBF8 as a homolog of CPBF1. CPBF1 was isolated as a potential receptor/carrier of the major virulence factor of *E. histolytica*, CP5, by virtue of its binding activity to CP5 (Nakada-Tsukui K, et al., unpublished data). CPBF8 represents a novel hydrolase receptor for the following reasons. First, CPBF8 is the first receptor that binds to and transport β-hexosaminidase α-subunit and lysozymes to lysosomes/phagosomes, in the manner that is distinct from mannose-6-phosphate receptor- and sortilin-dependent pathway. Second, there is no CPBF8 homolog in other organisms, and showed no sequence similarity to mannose-6-phosphate receptors or sortilin at the primary sequence level. Mannose-6-phosphate receptor and sortilin 1 are the membrane receptor of cathepsin D/β-hexosaminidase [47] and prosaponin/sphingolipid activator protein [48], respectively. Third, CPBF8 is post-translationally modified at its unique serine-rich region, and the modification is essential for the cargo binding.

Cellular localization of CPBF8

The two representative CPBF members, CPBF1 and CPBF8, are localized to distinct compartments in steady state. Immunofluorescence assay using two markers, LysoTracker and PNT, clearly showed distinct distribution of CPBF1 and CPBF8. CPBF8 was well colocalized with LysoTracker and PNT (Figure 1), whereas CPBF1 was seldom localized to lysosomes or colocalized with PNT (Nakada-Tsukui K, et al., unpublished data). The different localization of CPBF8 and CPBF1 may be attributable to the motif sequences at the carboxyl terminus. As mentioned above, the YxxL motif is located at the very end of the carboxyl terminus CPBF1, while CPBF8 ends with a stretch of YxxLA, suggesting a possibility that different accessory molecule(s) bind to CPBF 1 and CPBF8.

When CPBF1 and CPBF8 were recruited to phagosomes, the subdomain of the phagosomal membrane they first come in contact with, seems to be indistinguishable. CPBF8 (Figure 1A) and CPBF1 (Nakada-Tsukui K, et al., unpublished data) were recruited to the basolateral portion of the "phagocytic mouth", similar to the domain where phosphatidylinositol-3-phosphate is localized [35]. The fact that CPBF8 and *Eh*PNT colocalize in steady state and are simultaneously transported to phagosomes upon phagocytosis, suggests that similar trafficking pathway and